(Approche?) Panoramique sur les plasmas

de la basse à la haute pression

Thierry Belmonte

Institut Jean Lamour – UMR CNRS 7198 – Lorraine University

NANCY (France)

thierry.belmonte@univ-lorraine.fr

0. Introduction

Low and high pressure ?

Ne ~ 10^{13}-10^{14} cm^{-3} DBD

Ne ~ 10^{16}-10^{18} cm^{-3}

LAL

Ne ~ 10^{10}-10^{11} cm^{-3}

ECR

Latrasse et al., J. Microw. Pow. Elect. Energ. 51 (2017) 237

Ne ~ 10^{11}-10^{12} cm^{-3}

HF discharge

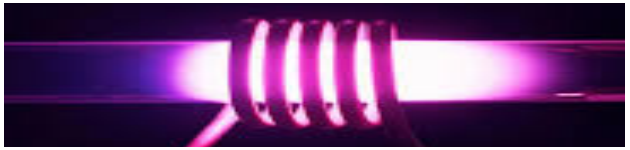

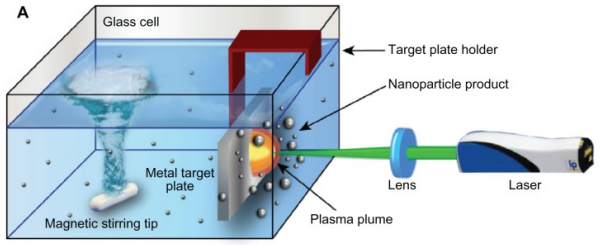

Zamiri *et al*. 2014 in "*Bioengineering Nanomaterials*", Ed. Tiwari & Tiwari, CRC press pp 269-290

10^0 10^1 10^2 10^3 10^4 10^5 10^6 10^7 10^8 Pa

10^{-2} 10^{-1} 10^0 10^1 10^2 10^3 10^4 10^5 10^6 mbar

Pressure

1 torr = 0.75 mbar

0. Introduction

Plasma or not plasma?

- Thermal or non thermal plasma? ⇨ Optical thickness?
- Reactive or non reactive plasma?
- Bounded or non bounded plasma? ⇨ Non neutral sheaths? Plasma-surface interaction?
- Multiphase? ⇨ Self-organization?

Pressure may play a role on possible applications:

- medicine (> atmospheric pressure)
- NPs (medium pressure for high purity, production rate and limited aggregation)
- sputtering / implantation (low pressure only)

0. Introduction

RF inductif dans l'argon

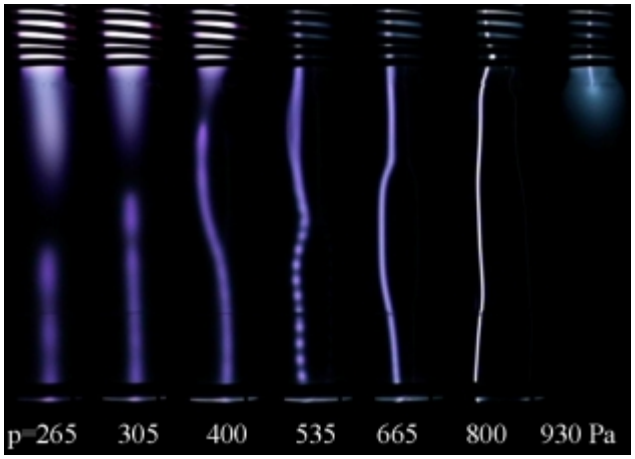

Crédit: P. Boubert & N. Bremard
http://plasmas.free.fr/rec/striations/striations.htm

Are effects due to pressure really complex?

Can we just change, in a software like Comsol for instance, the pressure value to simulate the « same » plasma?

1. What equilibrium predicts…

1. What equilibrium predicts…

Direct process	Reversible reaction	Reverse process
Collisional excitation	$A + e \leftrightarrow A^* + e$	(a) collisional de-excitation (or superelastic collision)
Collisional ionization	$A + e \leftrightarrow A^+ + e + e$	(b) 3-body recombination
Photoionization	$A + h\nu \leftrightarrow A^+ + e$	(c) Radiative recombination
Photoexcitation	$A + h\nu \leftrightarrow A^*$	(d) Spontaneous and stimulated emission

THERMODYNAMIC EQUILIBRIUM

Processes (a) to (d) occur in detailed balance

$$\frac{N_e N_i}{N_{i-1}} = \frac{g_e g_i}{g_{i-1}} \frac{(2\pi m_e k_B T)^{3/2}}{h^3} \times \exp\left(-\frac{E_i - E_{i-1}}{k_B T}\right)$$

Saha-Boltzmann distribution

$$\frac{N_u}{N_l} = \frac{g_u}{g_l} \times \exp\left(-\frac{E_u - E_l}{k_B T_{exc}}\right)$$

Maxwell-Boltzmann distribution

$$B_\nu(T) = 2h\frac{\nu^3}{c^2}\frac{1}{\exp\left(\frac{h\nu}{k_B T}\right) - 1}$$

Planck's function for the spectral radiance

$$f(v)\,dv = 4\pi\left(\frac{m_e}{2\pi k_B T_e}\right)^{3/2} \exp\left(\frac{-m_e v^2}{2k_B T_e}\right) v^2\,dv$$

Maxwellian distribution

1. What equilibrium predicts…

Direct process	Reversible reaction	Reverse process
Collisional excitation	$A + e \leftrightarrow A^* + e$	(a) collisional de-excitation (or superelastic collision)
Collisional ionization	$A + e \leftrightarrow A^+ + e + e$	(b) 3-body recombination
Photoionization	$A + h\nu \leftrightarrow A^+ + e$	(c) Radiative recombination
Photoexcitation	$A + h\nu \leftrightarrow A^*$	(d) Spontaneous and stimulated emission

Complete LOCAL THERMODYNAMIC EQUILIBRIUM

Processes (a) to (c) dominate processes (d)

$$\frac{N_e N_i}{N_{i-1}} = \frac{g_e g_i}{g_{i-1}} \frac{(2\pi m_e k_B T)^{3/2}}{h^3} \times \exp\left(-\frac{E_i - E_{i-1}}{k_B T}\right)$$

Saha-Boltzmann distribution

$$\frac{N_u}{N_l} = \frac{g_u}{g_l} \times \exp\left(-\frac{E_u - E_l}{k_B T_{exc}}\right)$$

Maxwell-Boltzmann distribution

~~$$B_\nu(T) = 2h\frac{\nu^3}{c^2}\frac{1}{\exp\left(\frac{h\nu}{k_B T}\right) - 1}$$~~

~~Planck's function for the spectral radiance~~

$$f(v)\,dv = 4\pi\left(\frac{m_e}{2\pi k_B T_e}\right)^{3/2} \exp\left(\frac{-m_e v^2}{2k_B T_e}\right) v^2\,dv$$

Maxwellian distribution

1. What equilibrium predicts…

Condition required to have complete LTE

1°) First proposal by Griem (assuming a homogeneous and time-independent plasmas)

$$N_e(\mathrm{cm}^{-3}) \geqslant 9.247 \times 10^{17} \left(\frac{k_B T_e}{E_H^i}\right)^{1/2} \left(\frac{E_2 - E_1}{E_H^i}\right)^3$$

For hydrogen, if Te = 1 eV $N_e > 1.0 \times 10^{17}\ \mathrm{cm}^{-3}$

Not realistic because in dense plasma, radiation does not escape freely as assumed here

2°) Second proposal by Griem

$$N_e(\mathrm{cm}^{-3}) \geqslant 10^{17} \left(\frac{k_B T_e}{E_H^i}\right)^{1/2} \left(\frac{E_2}{E_H^i}\right)^3$$

Resonant lines supposed to be optically thick

3°) Third proposal by Mc Whirter

$$N_e(\mathrm{cm}^{-3}) \geqslant 1.5 \times 10^{18} \left(\frac{T_e}{10^6}\right)^{0.55 - \left(\frac{0.49}{z}\right)^{3/2}}$$

For hydrogen, if Te = 1 eV $N_e > 6.0 \times 10^{17}\ \mathrm{cm}^{-3}$

4°) Fourth proposal by Christoforetti $N_e(cm^{-3}) > 1.6 \times 10^{12} T_e^{1/2} (\Delta E_{nm})^3$ may include Gaunt's factor

For hydrogen, if Te = 1 eV $N_e = 1.8 \times 10^{17} cm^{-3}$

1. What equilibrium predicts…

Direct process	Reversible reaction		Reverse process
Collisional excitation	$A^* + e \leftrightarrow A^{**} + e$	(a)	collisional de-excitation (or superelastic collision)
Collisional ionization	$A^* + e \leftrightarrow A^+ + e + e$	(b)	3-body recombination
Photoionization	$A^* + h\nu \leftrightarrow A^+ + e$	(c)	Radiative recombination

Partial LOCAL THERMODYNAMIC EQUILIBRIUM

Processes (a) to (c) dominate processes (d) but equilibrium is reached for high-energy levels only

$$\frac{N_e N_i}{N_{i-1}} = \frac{g_e g_i}{g_{i-1}} \frac{(2\pi m_e k_B T)^{3/2}}{h^3} \times \exp\left(-\frac{E_i - E_{i-1}}{k_B T}\right)$$

Saha-Boltzmann distribution (for level p to ion)

$$\frac{N_u}{N_l} = \frac{g_u}{g_l} \times \exp\left(-\frac{E_u - E_l}{k_B T_{exc}}\right)$$

Maxwell-Boltzmann distribution (for level p to ion)

The ASDF contains an upper side where high-energy levels are thermalized, following a Boltzmann distribution and related to the ion population by the Saha equation.

The lower side relates to low-energy levels that do not follow the Boltzmann-Saha equation.

The experimental determination of T_{exc} by Boltzmann's plot will give values different from T_e.

1. What equilibrium predicts…

Partial LOCAL THERMODYNAMIC EQUILIBRIUM

Ionizing and … recombining plasmas

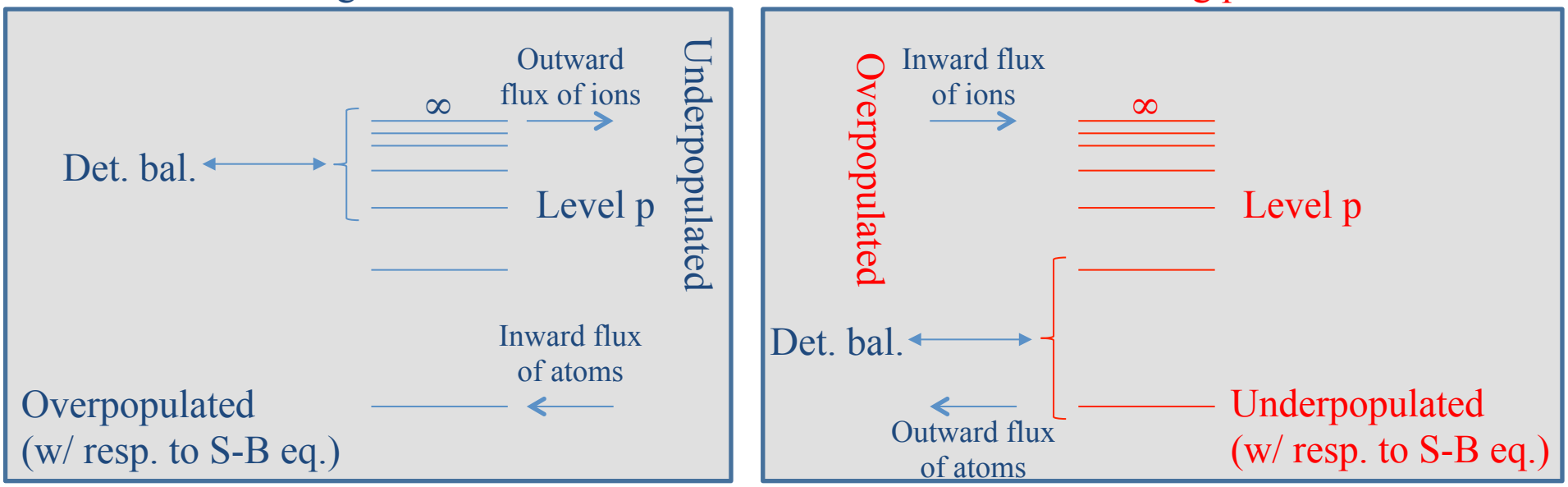

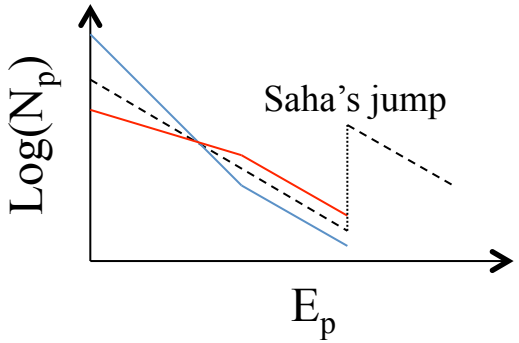

'Ionizing' plasmas: the lowest states of the ASDF are overpopulated with respect to the equilibrium, in agreement with the definition given by Fujimoto and McWhirter

1. What equilibrium predicts…

Reaching the same equilibrium state requires
a higher electron density when pressure rises

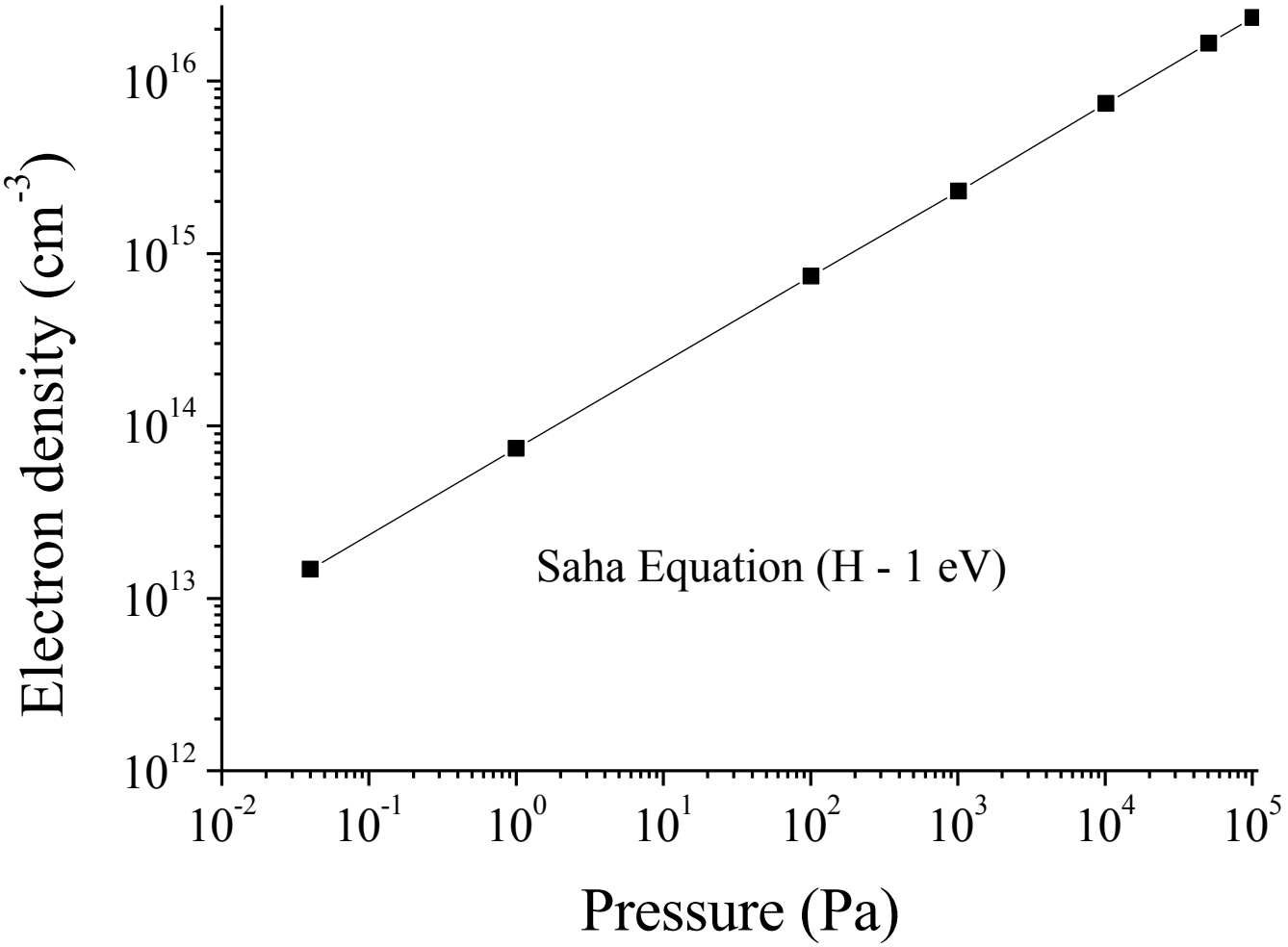

1. What equilibrium predicts…

The TIA (Torche à Injection Axiale)
Made to be used as a lamp.

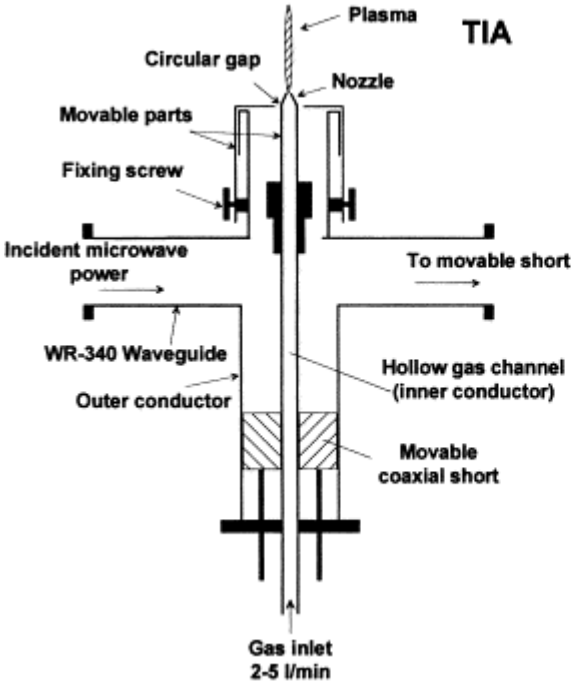

Moisan et al. Plasma Sources Sci. Technol. 3 (1994) 584

Intensively studied, even for thin film deposition at atmospheric pressure…

1. What equilibrium predicts…

Partial LOCAL THERMODYNAMIC EQUILIBRIUM

The ASDF contains an upper side with high-energy levels that are thermalized, following a Boltzmann distribution and related to the ion population by the Saha equation (in orange).

The lower side relates to low-energy levels that do not follow the Boltzmann-Saha equation.

Experimental determination of T_{exc} by Boltzmann's plot gives values different from T_e.

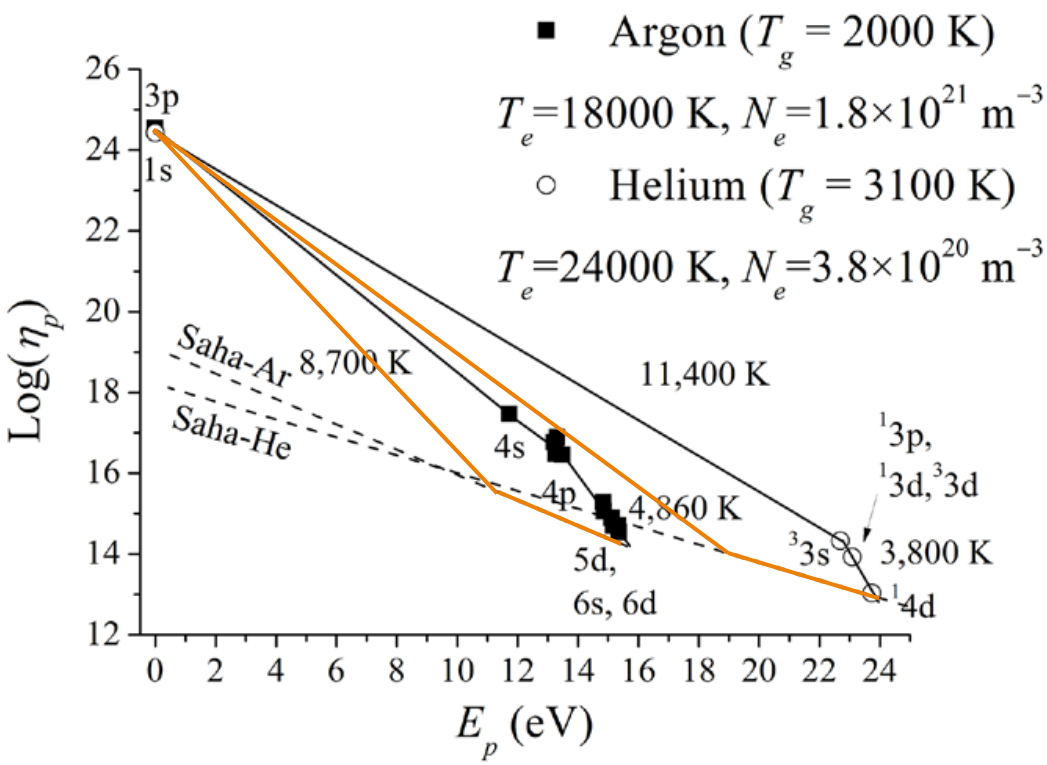

The atomic state distribution functions (ASDF) in helium and in argon for a 'torche a injection axiale' (TIA). After Jonkers *et al* (1996). $\eta_p=N_p/g_p$.

1. What equilibrium predicts…

Condition required to have partial LTE

1°) Proposal by Griem:

$$N_e(\mathrm{cm}^{-3}) \geqslant \frac{10}{2\sqrt{\pi}} \left(\frac{e^2}{a_0^2 4\pi\varepsilon_0 \hbar c} \right) \frac{z^7}{p^{17/2}} \left(\frac{k_B T_e}{E_{H^z}^i} \right)^{1/2}$$

For hydrogen, if T_e = 1 eV, taking p=2 $\quad N_e > 5.5 \times 10^{15}\ \mathrm{cm}^{-3}$

2°) Minimum time required to reach equilibria. After Griem:

$$\tau_{rel} \approx 1.151 \times 10^{13} \frac{\alpha}{f_{12} N_e} \frac{E_2}{E_H^i} \left(\frac{k_B T_e}{E_H^i} \right)^{1/2} \exp\left(\frac{E_2}{k_B T_e} \right)$$

For hydrogen, if $N_e \sim 10^{16}$ cm^{-3}, T_e = 1 eV, $\tau_{rel} \sim 3.2$ µs

(At 10^{15} cm^{-3}: x τ by 10)

For argon, $\tau_{rel} \sim 182$ µs

τ depends strongly on the enery level of the first excited state: the lowest, the shortest

1. What equilibrium predicts…

The partition function is the sum of several terms:

$$Q_{tot} = Q_{trans} + \underbrace{Q_{int}}_{Q_{elec}+Q_{vib}+Q_{rot}} + Q_{reac}$$

$$Q_{trans} = \left(\frac{2\pi m k_B T}{h^2}\right)^{3/2} \frac{k_B T}{P}$$

For atoms: $Q = Q_{int} = \sum_{j=1}^{p} g_{j(n,l,s)} \exp\left(\frac{-E_j(n,l,s)}{k_B T}\right)$ Cannot be extended to infinity!

How to choose p?

1°) no Rydberg states' mean radius should exceed the mean distance between particles

$$n_{max} \approx 30\sqrt{z}\,(N/10^{21})^{-1/6}$$

2°) Lowering of the ionization potential

1. What equilibrium predicts…

Lowering of the ionization potential

Debye-Hückel theory

Ritz-Rydberg distribution

$$E_p = E_i - \frac{Ry}{\left(p + A + \frac{B}{p^2}\right)^2} \quad ; \quad p < p_{max}$$

At $p=p_{max}$, $E_i < E_i^{ref}$-ΔE^{ion}

$$\Delta E^{ion} = \frac{ze^2}{4\pi\varepsilon_0\lambda_D}$$

For H, at 1 atm and 1 eV $\Delta E^{ion} = 0.154\,\text{eV}$, and p_{max}~10

1. What equilibrium predicts…

Lowering of the ionization potential

$\Delta E^{ion} > 0.9$ eV (i.e. $\sim 10^{19}$ cm^{-3})

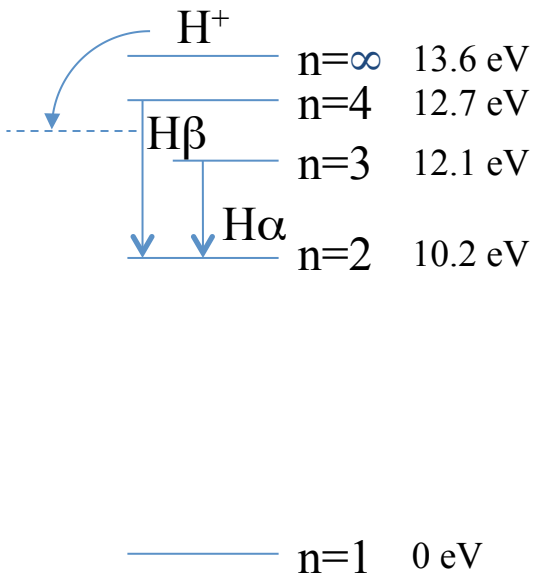

No Hβ, γ, etc.

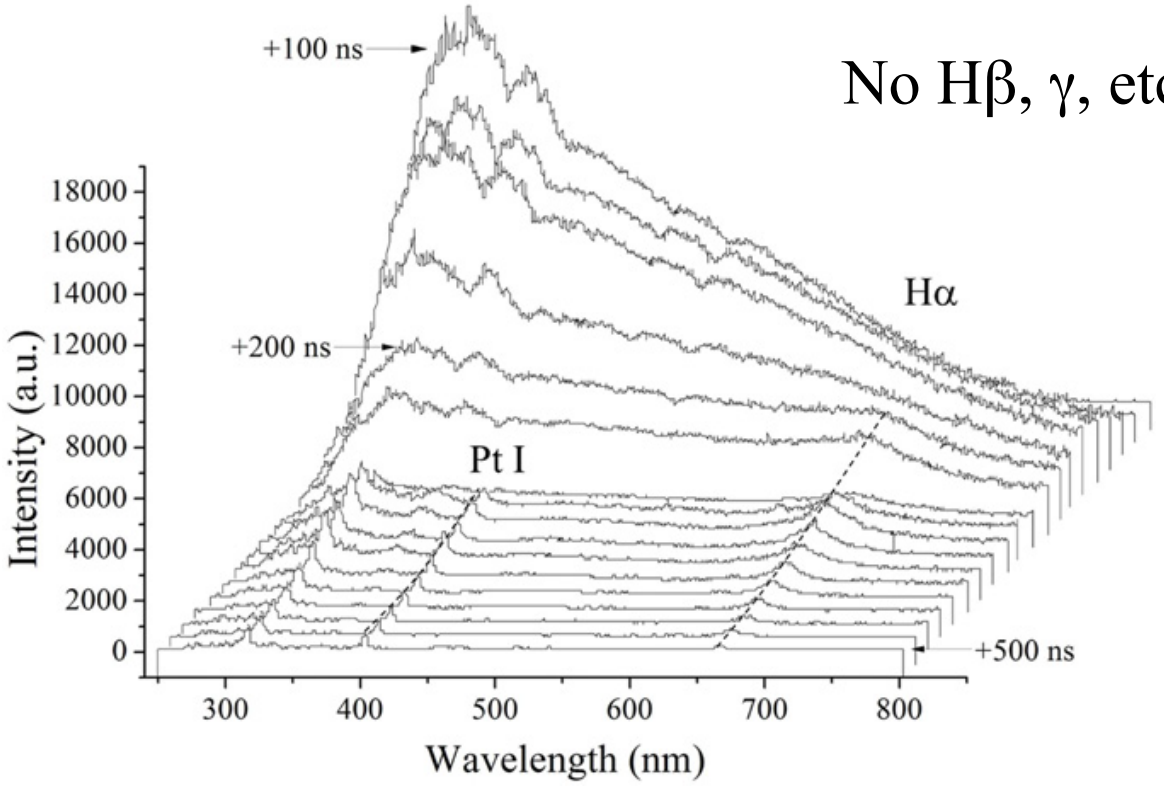

Time-resolved OES in heptane between 2 Pt electrodes

2. Excimers, ions and ambipolar diffusion

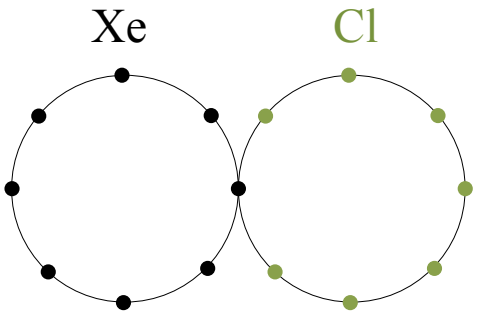

2. Excimers, ions and ambipolar diffusion

Example of He plasmas

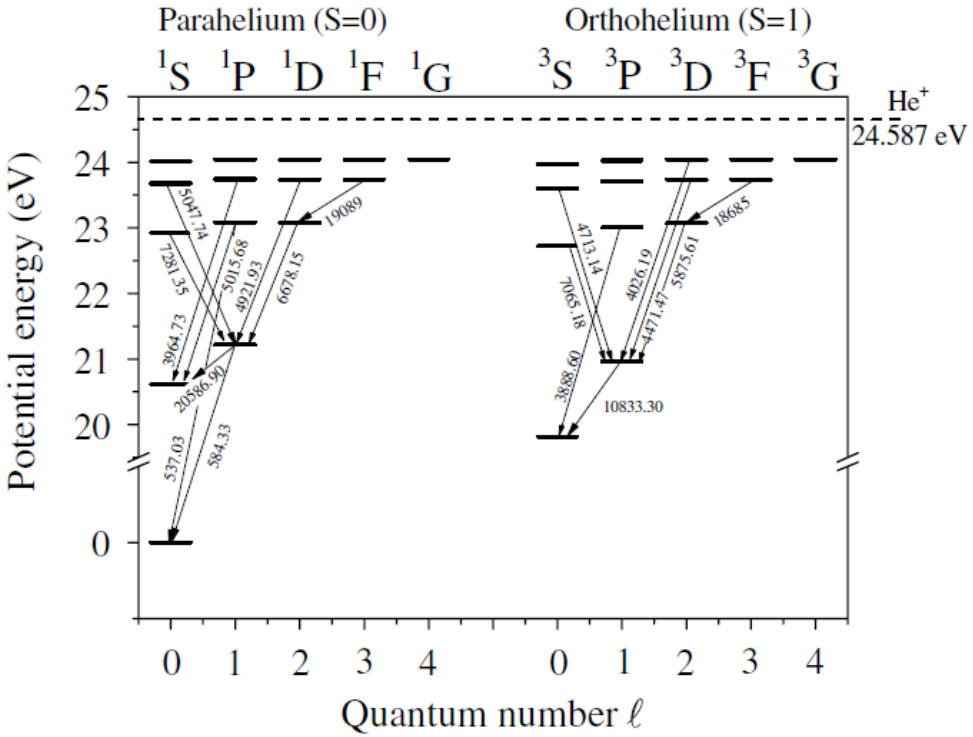

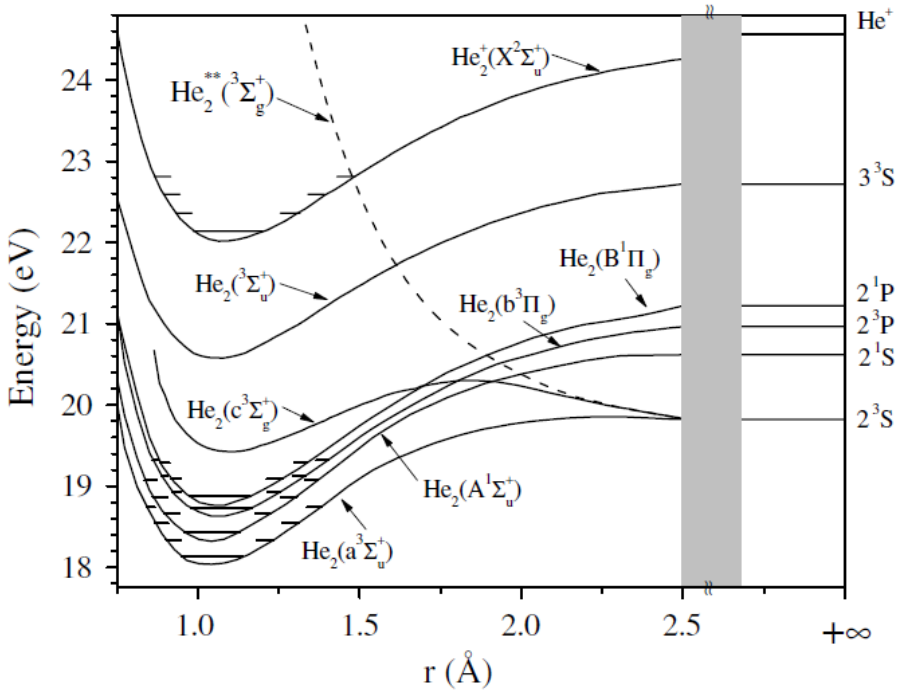

2. Excimers, ions and ambipolar diffusion

Institut Jean Lamour

Example of He plasmas

Ionization

1	$He + e \longrightarrow He^+ + e + e$		$1.5 \times 10^{-9} \hat{T}_e^{0.68} \exp\left(-\frac{24.6}{\hat{T}_e}\right)$
2	$\begin{Bmatrix} He(2^1P) \\ He(2^3P) \\ He(2^1S) \\ He(2^3S) \end{Bmatrix} + e \longrightarrow He^+ + e + e$	$\begin{Bmatrix} 19\% \\ 56\% \\ 6\% \\ 19\% \end{Bmatrix}$	$1.28 \times 10^{-7} \hat{T}_e^{0.6} \exp\left(-\frac{4.78}{\hat{T}_e}\right)$
3	$He_2^* + e \longrightarrow He_2^+ + e + e$		$9.75 \times 10^{-10} \hat{T}_e^{0.71} \exp\left(-\frac{3.40}{\hat{T}_e}\right)$
4	$He(2) + He(2) \longrightarrow \begin{Bmatrix} He^+ + He + e \\ He_2^+ + e \end{Bmatrix}$	$\begin{Bmatrix} 30\% \\ 70\% \end{Bmatrix}$	1.5×10^{-9}
			$\begin{Bmatrix} 2.7 \times 10^{-10} \\ — \end{Bmatrix}$
5	$He(2) + He_2^* \longrightarrow \begin{Bmatrix} He^+ + He + He + e \\ He_2^+ + He + e \end{Bmatrix}$	$\begin{Bmatrix} 30\% \\ 70\% \end{Bmatrix}$	$2.9 \times 10^{-9} \left(\frac{T_g}{300}\right)^{0.5}$
		$\begin{Bmatrix} 15\% \\ 85\% \end{Bmatrix}$	1.5×10^{-10}
		$\begin{Bmatrix} 15\% \\ 85\% \end{Bmatrix}$	2.5×10^{-9}
6	$He(3) + e \longrightarrow He^+ + e + e$		
7	$\begin{Bmatrix} He(3^1S) \\ He(3^1P) \\ He(3^1D) \\ He(3^3S) \\ He(3^3P) \\ He(3^3D) \end{Bmatrix} + He \longrightarrow He_2^+ + e$		2.90×10^{-10} 8.60×10^{-12} 2.30×10^{-10} 2.90×10^{-11} 3.40×10^{-11} 3.60×10^{-11}
8	$He(4) + e \longrightarrow He^+ + e + e$		
9	$\begin{Bmatrix} He(4^3S) \\ He(4^1S) \\ He(4^3P) \\ He(4^3D) \\ He(4^1D) \\ He(4^3F) \\ He(4^1F) \\ He(4^1P) \end{Bmatrix} + He \longrightarrow He_2^+ + e$		3.80×10^{-11} 3.40×10^{-11} 7.80×10^{-11} 1.50×10^{-10} 2.50×10^{-10} 1.10×10^{-10} 2.00×10^{-10} 4.20×10^{-11}
		$\begin{Bmatrix} 15\% \\ 85\% \end{Bmatrix}$	1.5×10^{-9}
10	$He_2^* + He_2^* \longrightarrow e + \begin{Bmatrix} He^+ + 3He \\ He_2^+ + 2He \end{Bmatrix}$	$\begin{Bmatrix} 15\% \\ 85\% \end{Bmatrix}$	2.7×10^{-10}
			$\begin{Bmatrix} — \\ 1.5 \times 10^{-9} \end{Bmatrix}$

No three-body process
= « same » importance what ever the pressure

Excimer production

26	$He^+ + He + He \longrightarrow He_2^+ + He$	1.0×10^{-31}
	$He_2^+ + He \longrightarrow He^+ + He + He$	$\frac{1.40 \times 10^{-6}}{T_g^{0.67}} \exp\left(-\frac{28100}{T_g}\right)$
27	$He(2^3P) + He + He \longrightarrow He_2^* + He$	1.6×10^{-32} 1.3×10^{-33} 1.6×10^{-32} for $He_2\ (A^1\Sigma_u^+)$
	$He_2^* + He \longrightarrow He(2^3P) + He + He$	3.6×10^{-14}
28	$He(2^3S) + He + He \longrightarrow He_2^* + He$	1.5×10^{-34} 1.3×10^{-33} 2.0×10^{-34} for all He^m 2.0×10^{-34}

three-body processes
= enhanced at high pressure

Be careful: autoionization of Rydberg states!

$$He_2^+(J, v) + e \rightarrow \{He_2^*; He_2^{**}\} \rightarrow He^* + He$$

Autoionization

Example of He plasmas

Pressure dependence of chemical reactions (falloff transition)

$$\frac{d[CH_4]}{dt} = k[H][CH_3][He] = k^M[H][CH_3]$$

k^M changes between
- a low-pressure constant k_0^M and
- a high-pressure constant k_∞^M

$$\frac{k_0^M[M]}{k_\infty^M} = \frac{[M]}{[M]_c}$$

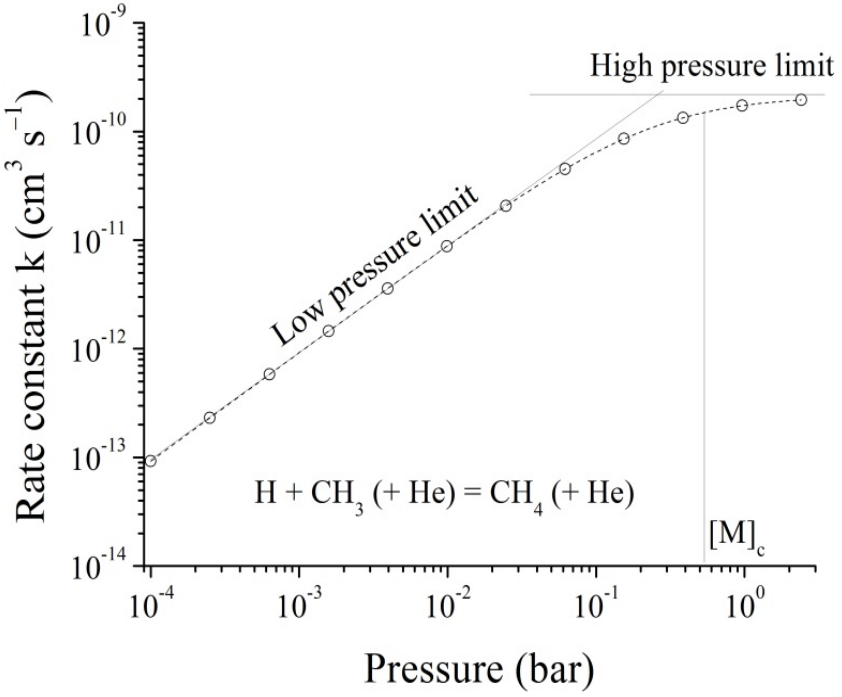

2. Excimers, ions and ambipolar diffusion

Example of He plasmas

Other significant excimers (dixit J.-M. Pouvesles, see J. Chem Phys. 76 (1982) 4006)

like He_3^+ and He_4^+ (mainly in cryogenic plasma)

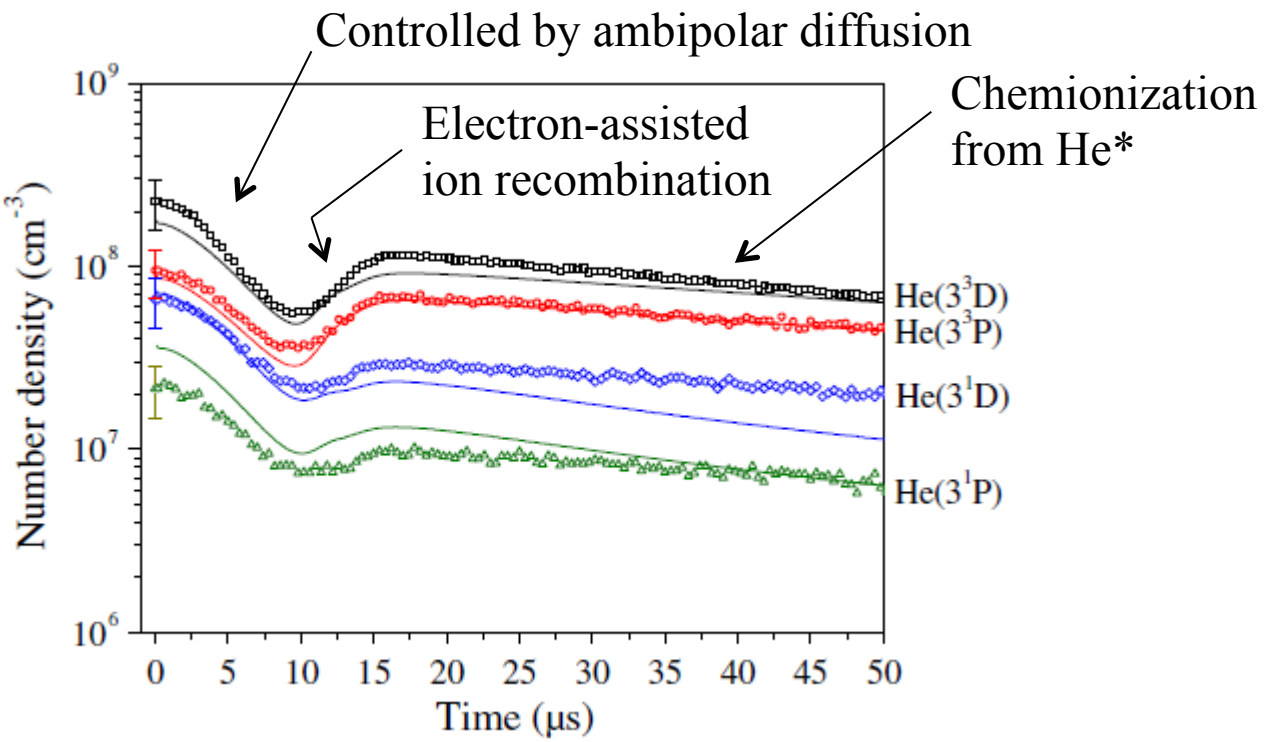

Time afterglow of a microwave He plasma at atmospheric pressure

2. Excimers, ions and ambipolar diffusion

Example of He plasmas

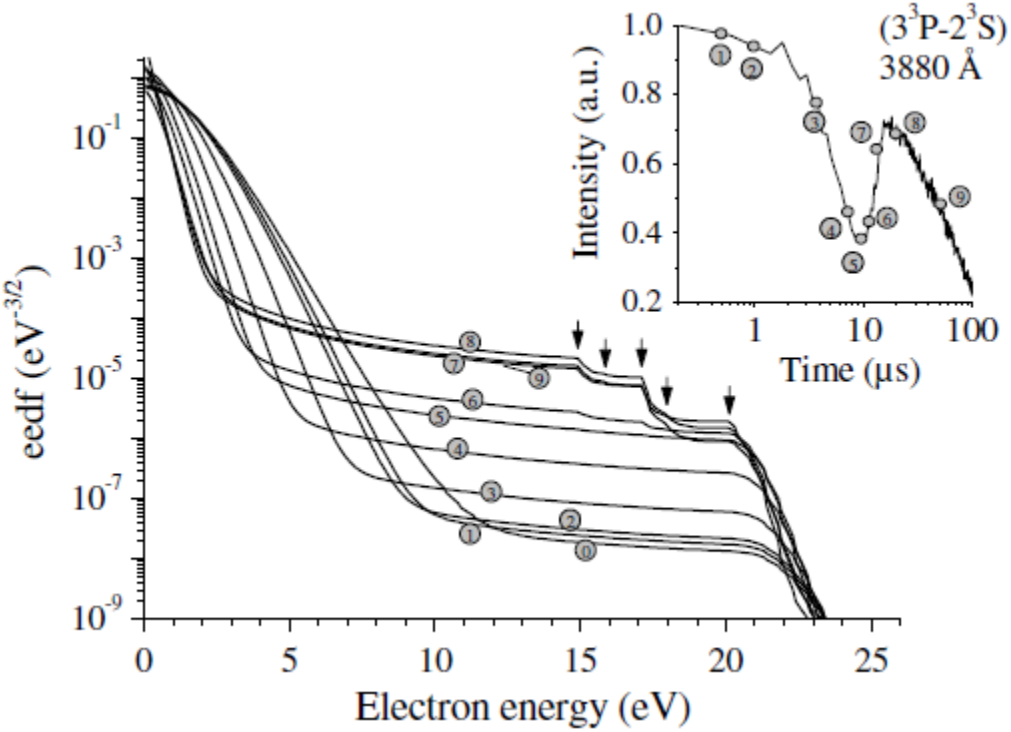

Predicted evolution of the electron energy distribution function at different stages in the post-discharge (label 0 refers to the steady state eedf). Each stage is referred to in the inset showing the evolution of one optical transition in post-discharge. Arrows indicate the energy of electrons created by chemionization that heats the eedf in late post-discharge. These arrows are located at 15.05, 15.85, 17.24, 18.04 and 20.04 eV.

Ambipolar diffusion and field

If the electron density in an electrically neutral plasma varies (perturbation, attachement, …), the resulting density gradient induces an excess of local positive ions.

This creates a local space charge field (the ambipolar field) and thus a backward force on electrons. Ions start moving faster (ion heating) whereas electrons are slowed down.

$$\vec{E}_a = \frac{D_e - \frac{n_i}{n_e} D_i}{\mu_e - \frac{n_i}{n_e} \mu_i} \nabla.\ln(n_e) \approx \frac{D_e - D_i}{\mu_e - \mu_i} \nabla.\ln(n_e)$$

High density is required
= mainly at high pressure

$$D_a = \frac{\mu_i D_e - \mu_e D_i}{\mu_i - \mu_e} \approx D_i \left(1 + \frac{T_e}{T_i}\right)$$

The ambipolar field must be included in the Boltzmann equation !

Ambipolar diffusion and field

The example of streamer propagation

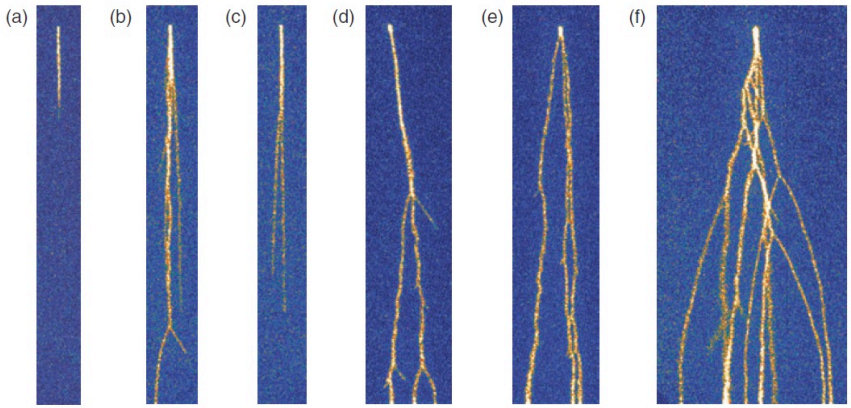

Images CCD d'une décharge pointe-plan dans l'air à différente tension appliquée (a) : 9 kV, (b)-(c) : 10 kV, (c)-(f) :12,5 kV. Cf van Veldhuizen and Rutgers, J. Phys. D: Appl. Phys., 35 (2002) 2169

Ambipolar diffusion and field

Example: streamer propagation

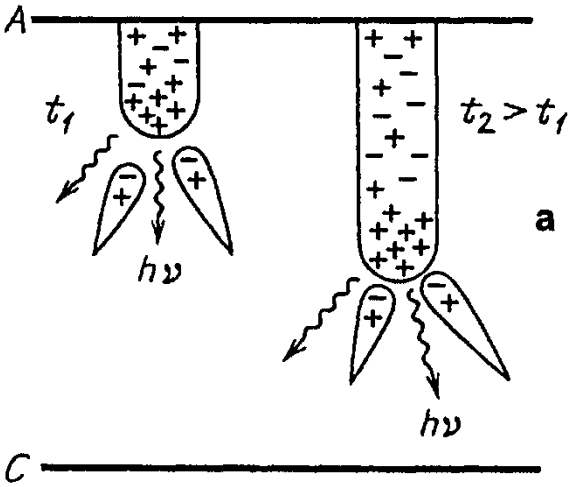

Dévelopement temporel d'un streamer positif.
Y P Raizer, (1991) "Gas Discharge Physics", Ed. par Springer-Verlag, Berlin

Be careful, ions are quasi-static within the gap.
Only electrons move.

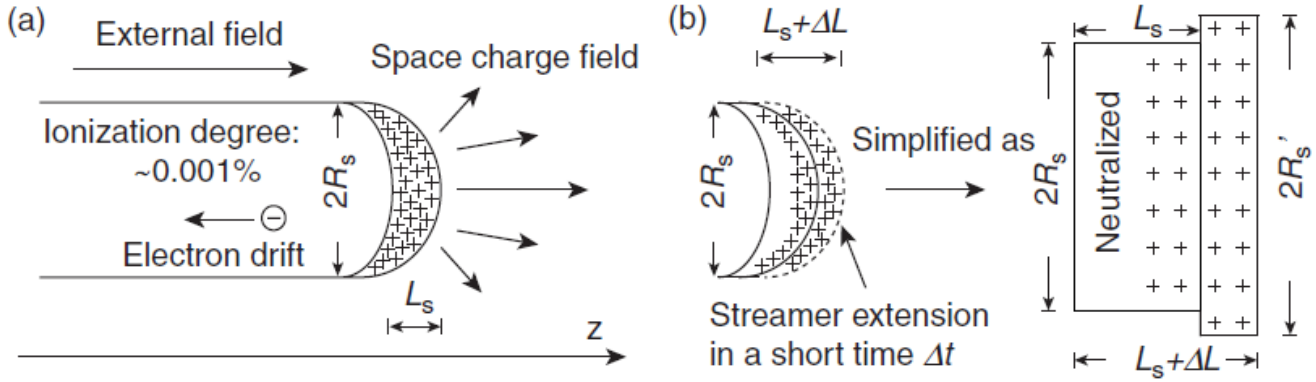

Qin & Pasko, J. Phys. D: Appl. Phys. **47** (2014) 435202

Ambipolar diffusion and field

1°) Avalanche

2°) Once N_e in the avalanche is so large that $E_{sc} \sim E_0$, the avalanche-to-streamer transition occurs

3°) The space charge strongly enhances E to values about 3–7 times E_{bd} in the region just ahead of the streamer, while screening the ambient field out of the streamer channel.

4°) The intense electron impact ionization in the high field region rapidly raises N_e, leading to the extension of the streamer into a new region = *space charge waves*, which can penetrate into neutral gas with a velocity much higher than the electron drift velocity, up to a fraction of the speed of light.

5°) As a new section of the streamer head is created as part of the previous streamer head is neutralized by the secondary electrons drifted backward from the new section of the positive streamer.

2. Excimers, ions and ambipolar diffusion

Ambipolar diffusion and field

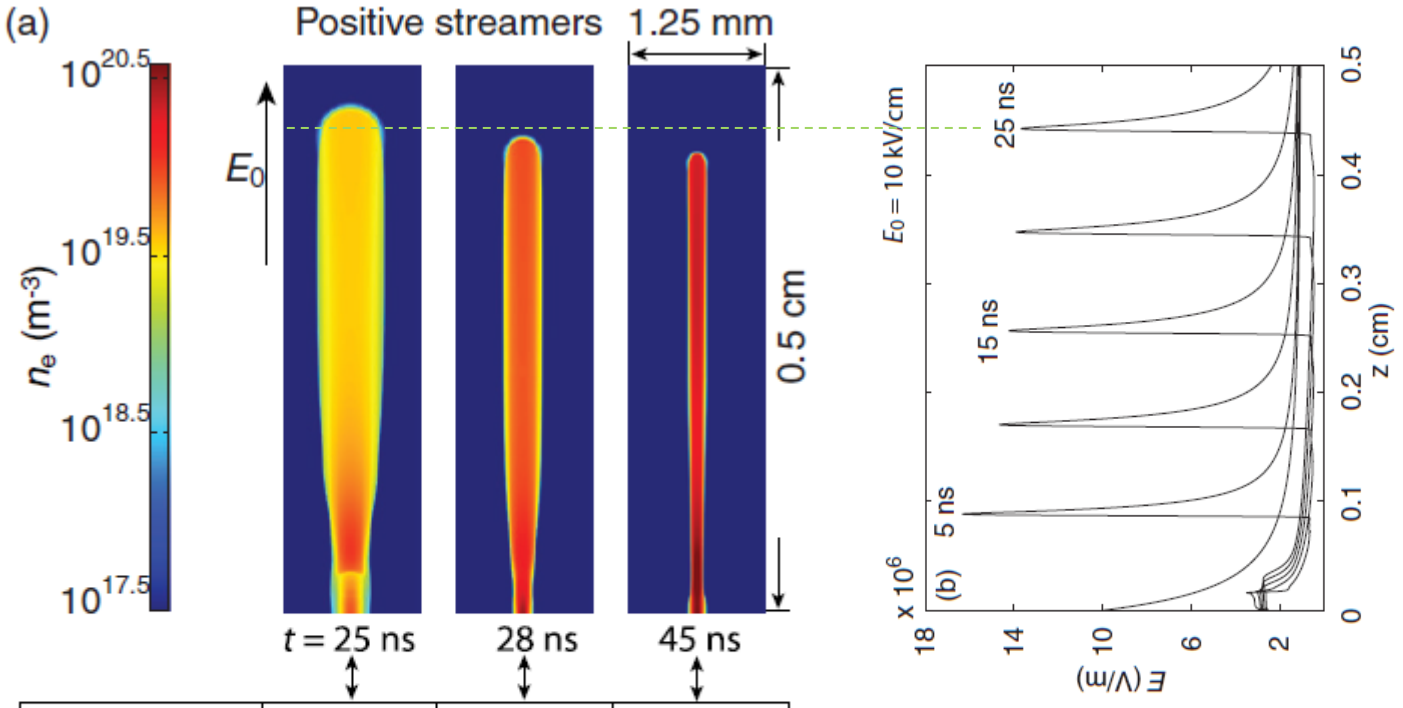

E_0 (kV/cm)	5.0	10.0	20.0
R_s (mm)	0.278	0.110	0.052
E_s / E_k	4.05	5.11	7.12
v_s (×10^5 m/s)	1.59	1.59	0.93
w_e (eV)	115.6	103.0	98.6
$C_0 = q_e E_0 R_s / w_e$	1.20	1.07	1.05

Qin & Pasko, J. Phys. D: Appl. Phys. **47** (2014) 435202

Ambipolar diffusion and field

Ambipolar diffusion with multiple ions:

- Electronegative gases (*e.g.* Cl_2 or SF_6)
- Dusty plasmas

3. Observing and probing

3. Observing and probing

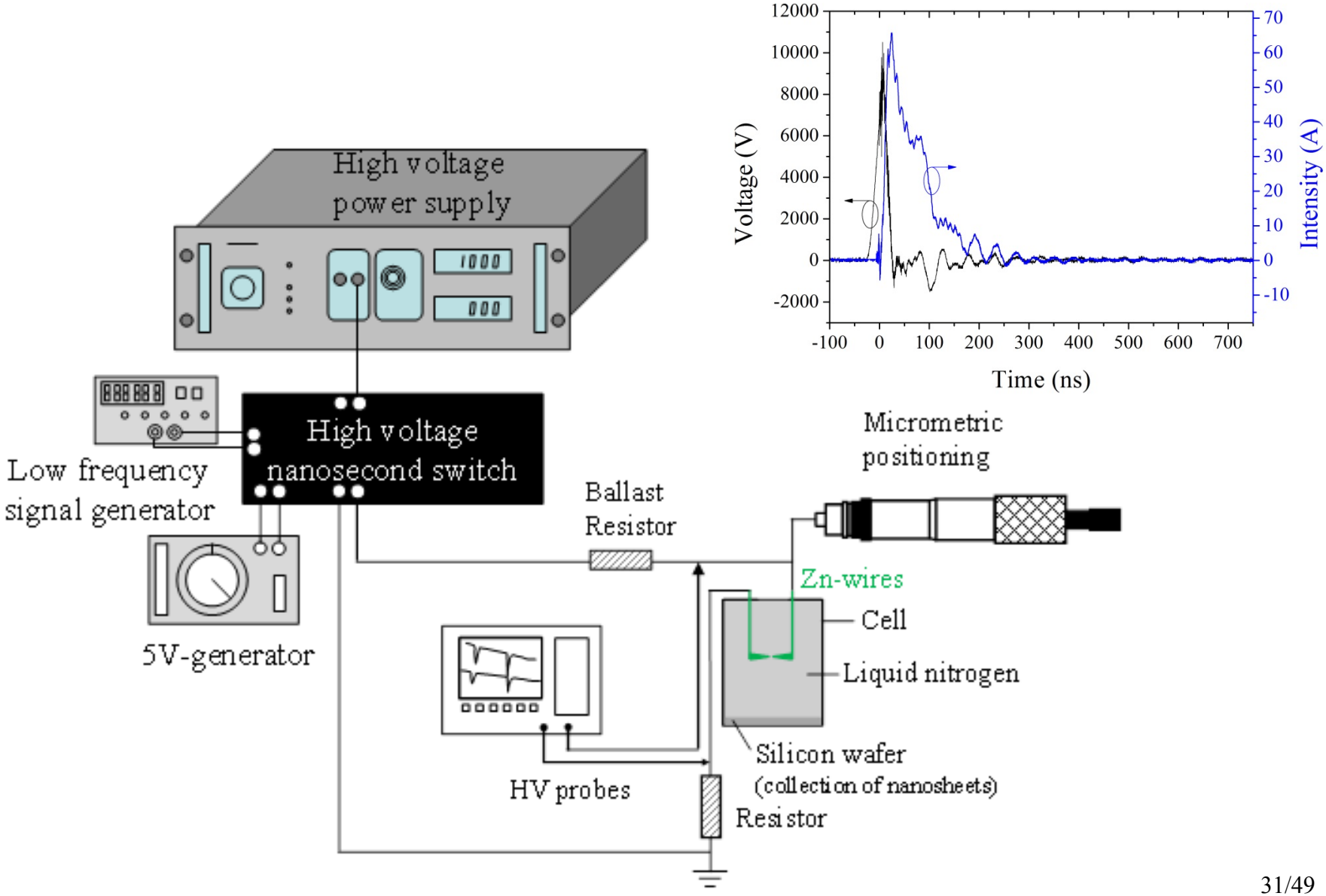

3. Observing and probing

High pressure prevents light from leaving and entering the medium

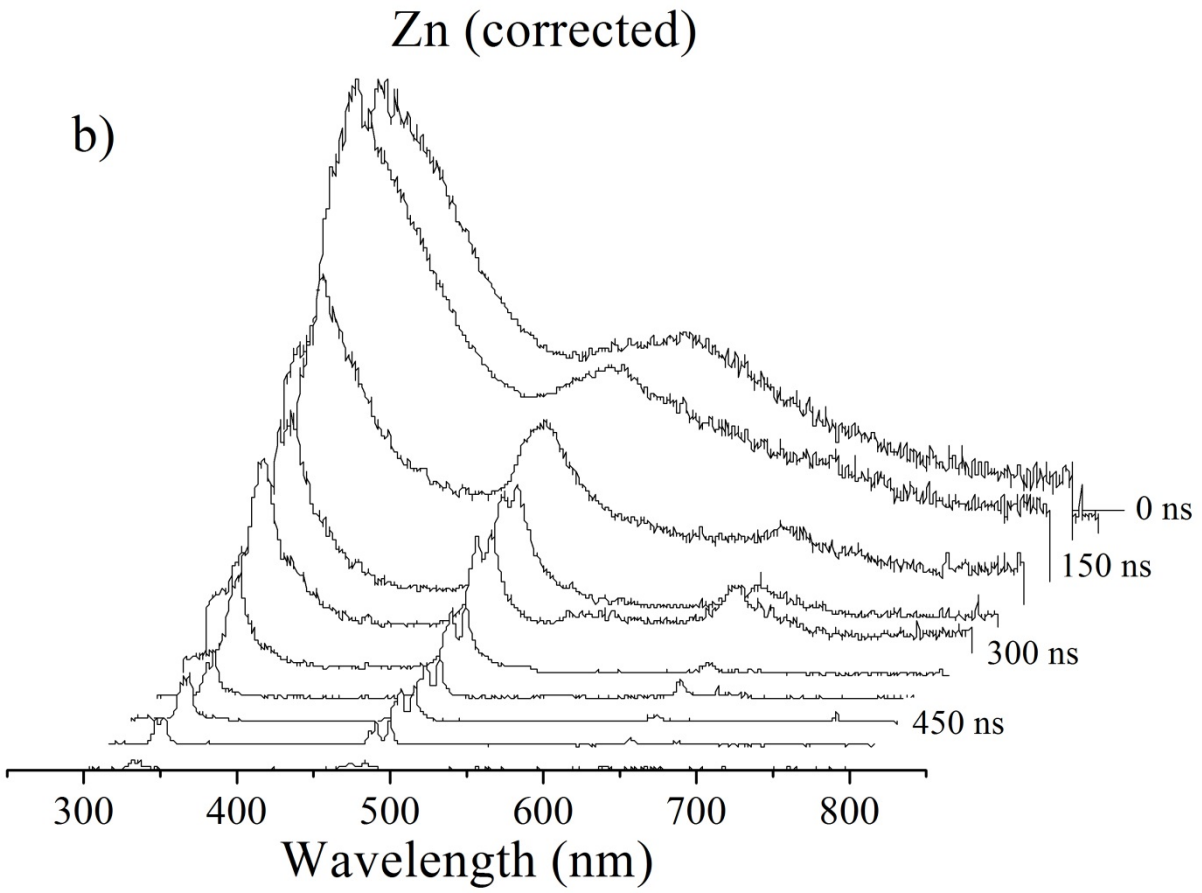

3. Observing and probing

Background emission at early stages

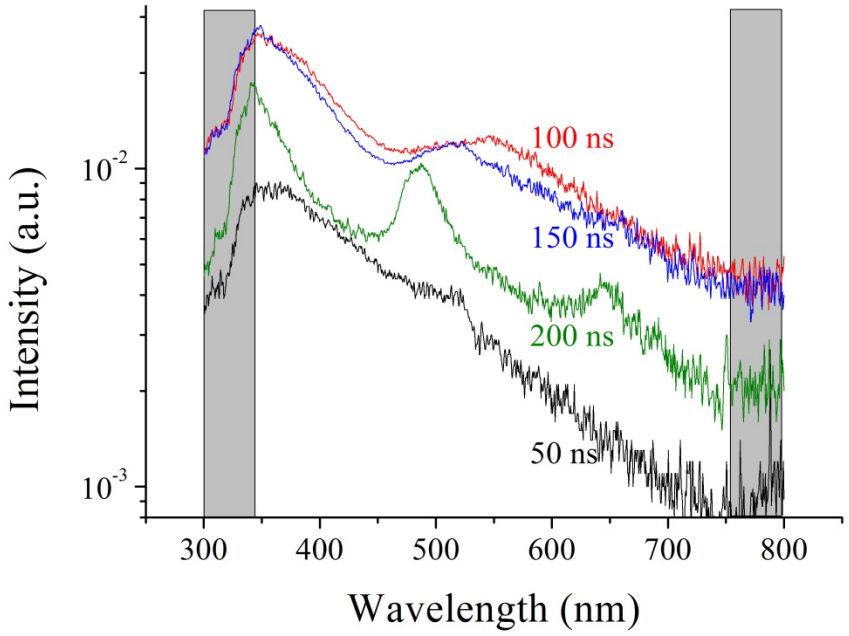

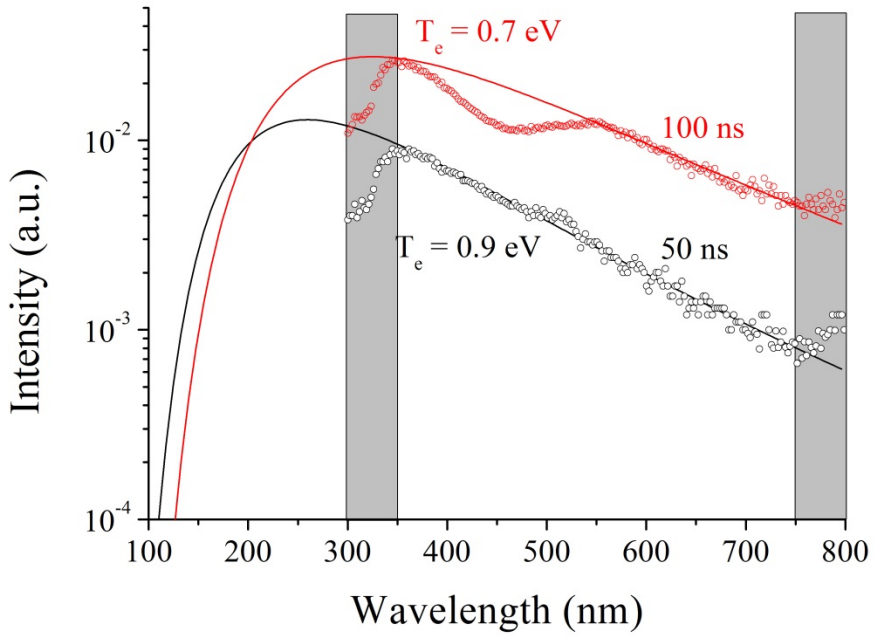

Case of some Zn emission lines

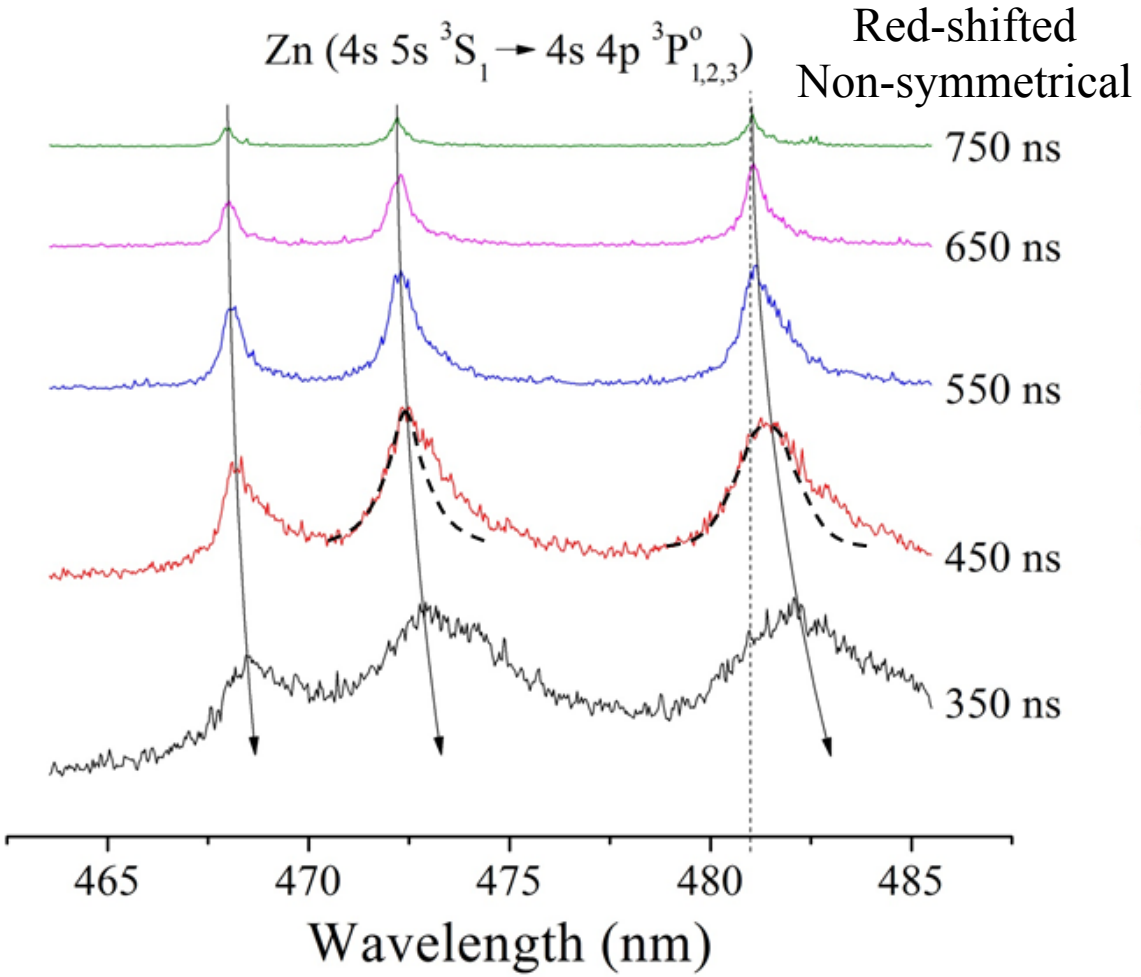

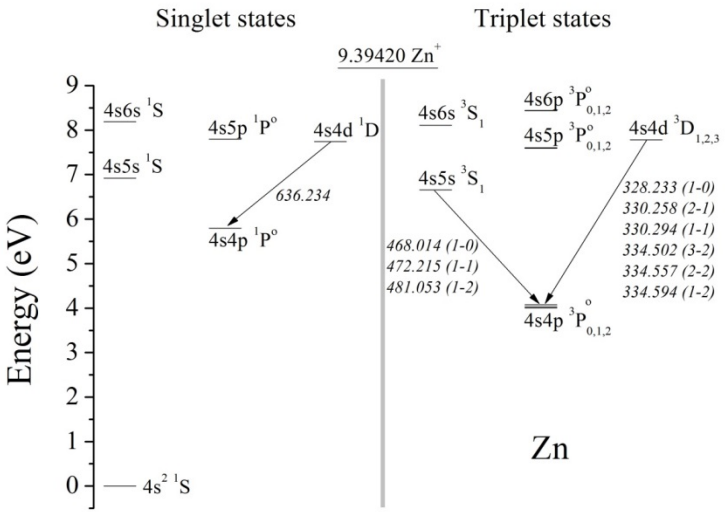

3. Observing and probing

When pressure gradients change the way light propagates

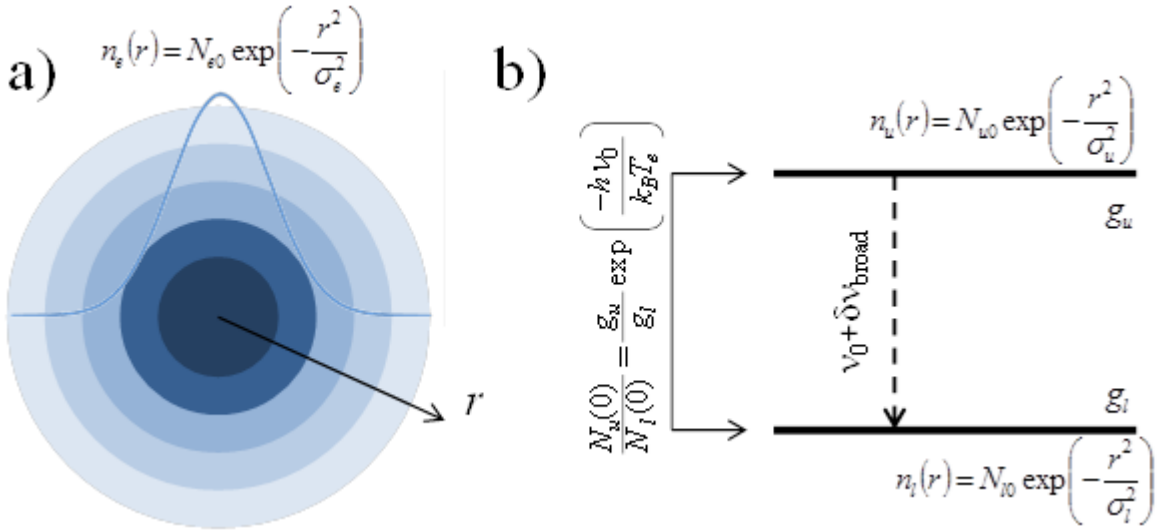

For a cylindrical plasma, the optical depth is defined as:

$$\tau \approx 2\pi \int_x^{r_p} \frac{c^2}{h\nu^3}\left[\exp\left(\frac{h\nu}{k_B T}\right) - 1\right]\frac{r}{\sqrt{r^2 - x^2}}\varepsilon \, dr$$

It must be doubled if a mirror is used
to double the optical path

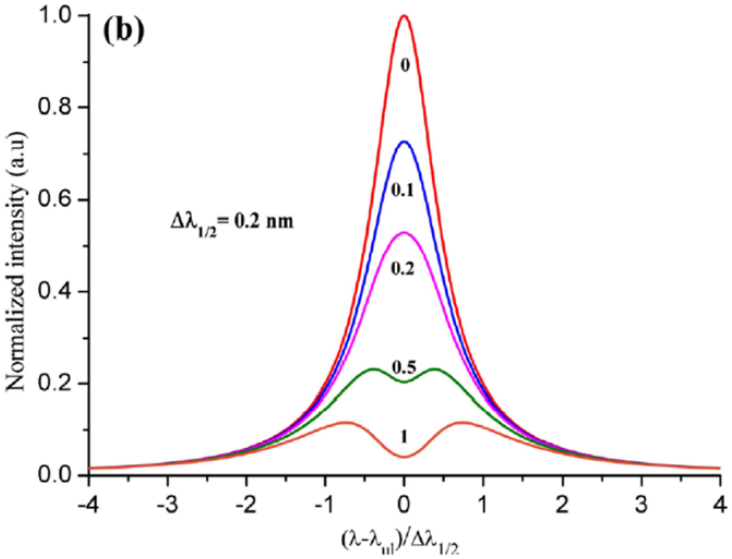

Differential Radiative Transfer equation (RTE)

Intensity of radiation
(at frequency ν along the line of sight (Ox) at point x)
[W sr^{-1} m^{-2} Hz^{-1}]

Spectral emission coefficient
(i.e. the power radiated at point x per unit solid angle, volume and frequency)
[W sr^{-1} m^{-3} Hz^{-1}]

$$\frac{1}{\kappa(\nu,x)}\frac{\mathrm{d}I(\nu,x)}{\mathrm{d}x} = -I(\nu,x) + \frac{\varepsilon(\nu,x)}{\kappa(\nu,x)}$$

Absorption coefficient [m^{-1}]

Optical depth: $\mathrm{d}\tau = -\kappa(\nu,x)\mathrm{d}x$

$$\frac{\mathrm{d}I(\nu,x)}{\mathrm{d}\tau} = I(\nu,x) - S(x)$$

$$\kappa(\nu,x) = \frac{h\nu}{c}[B_{lu}N_l(x) - B_{ul}N_u(x)]S(x,\nu)$$

$$\varepsilon(\nu,x) = \frac{h\nu}{4\pi}A_{ul}N_u(x)S(x,\nu),$$

$S(x) = \varepsilon(\nu, x)/\kappa(\nu, x)$ is called as the source function

3. Observing and probing

Institut Jean Lamour

Self-reversal of Al emission line profile

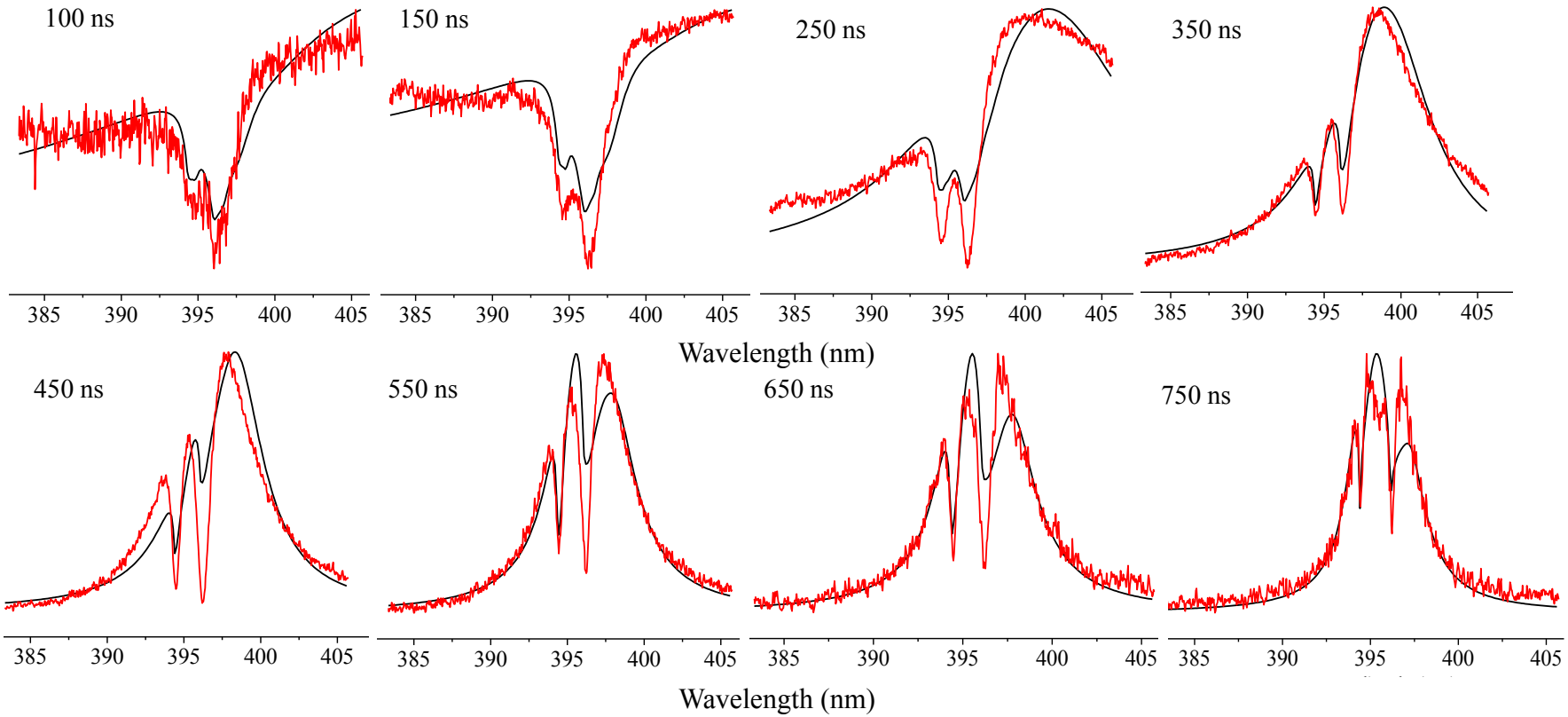

Continua: Planck's continuum

Planck's law

The emissivity expressed in radiated by a plasma at a temperature T is related to the Planck law by the Kirchhoff law

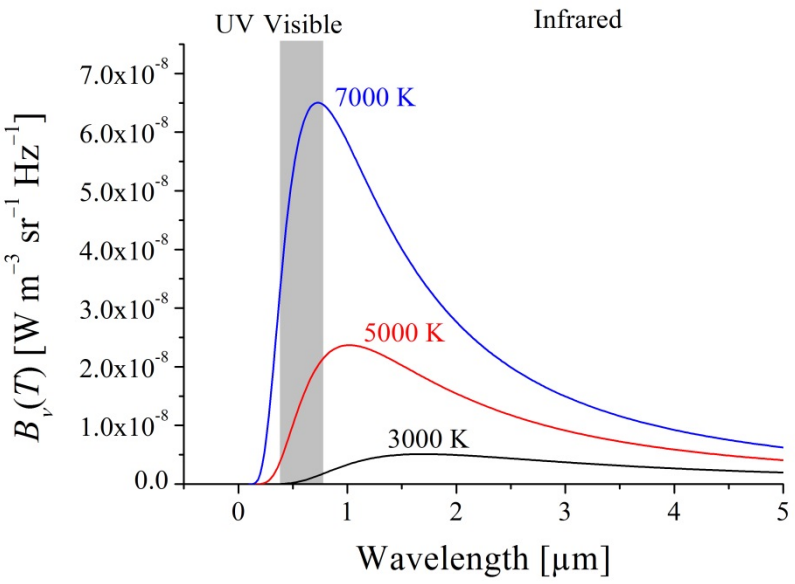

Absorption coefficient (m^{-1})

$$\varepsilon_P(\nu, T) = \kappa_P(\nu, T) B_\nu(T)$$

Emissivity ($W\ m^{-3}\ sr^{-1}\ Hz^{-1}$)

Intensity of radiation ($W\ m^{-2}\ sr^{-1}\ Hz^{-1}$)

$$B_\nu(T) = \frac{2h\nu^3}{c^2} \frac{1}{\exp\left(\frac{h\nu}{k_B T}\right) - 1}$$

The Planck continuum is composed of a large number of individual emission lines

For one of these lines:

$$\kappa_P^{u \to l}(T) = \frac{h\nu}{c} \phi(\nu)(N_l B_{lu} - N_u B_{ul})$$

3. Observing and probing

Continua: e-i recombination

g_{fb} is the free–bound Gaunt factor
It accounts for the misfit
between quantum–classical predictions

Free-bound transitions

$$X^{i+} + e \rightarrow X_p^{(i-1)+} + h\nu \qquad \text{direct}$$

$$X_p^{(i-1)+} + h\nu \rightarrow X^{i+} + e \qquad \text{reverse}$$

$$\sigma_{\nu p} = \frac{1}{(4\pi\varepsilon_0)^5} \frac{2^7\pi^4 e^{10}}{3\sqrt{3} \times m_e c^3 h^4} \frac{Z^4}{\nu} \frac{g_{fb}}{p^3 v_e^2}$$

Emissivity due to the recombination process

$$\varepsilon_{R,p}^{ei}(\nu, T_e)\mathrm{d}\Omega\,\mathrm{d}\nu = \frac{\mathrm{d}\Omega\,\mathrm{d}\nu}{4\pi} \int_0^\infty h\nu\, N_e N_i f(v_e) v_e \sigma_{\nu p}\, \mathrm{d}v_e$$

For a maxwellian vdf

$$\varepsilon_{R,p}^{ei}(\nu, T_e)\,\mathrm{d}\nu\,\mathrm{d}\Omega = \frac{1}{(4\pi\varepsilon_0)^2} \frac{16e^4 h}{3m_e^2 c^3\sqrt{3\pi}} \left(\frac{Ry}{k_B T_e}\right)^{3/2} N_e N_i \frac{Z^4}{p^3}\, \bar{g}_{fb} \exp\left(-\frac{h\nu}{k_B T_e}\right) \exp\left(\frac{Z^2 Ry}{p^2 k_B T_e}\right) \mathrm{d}\nu\,\mathrm{d}\Omega,$$

$\bar{g}_{fb}$: thermally averaged free–bound Gaunt factor (averaged over vdf)

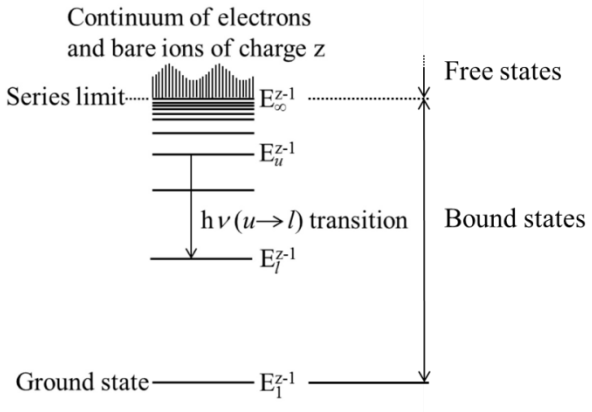

Need for summation over bound states

$$\varepsilon_R^{ei}(\nu, T_e) = \sum_{p \geq \sqrt{\frac{Z^2 Ry}{h\nu}}}^{p^*} \varepsilon_{R,p}^{ei}(\nu, T_e) + \sum_{p^*+1}^{\infty} \varepsilon_{R,p}^{ei}(\nu, T_e)$$

Continua: bremsstrahlung

Because high levels are close to each other

$$\sum_{p^*+1}^{\infty} \frac{1}{p^3} \exp\left(\frac{Z^2 \mathrm{Ry}}{p^2 k_\mathrm{B} T_\mathrm{e}}\right) = -\frac{1}{2} \int_{1/(p^*+1)^2}^{0} \exp\left(\frac{Z^2 Ry}{p^2 k_\mathrm{B} T_\mathrm{e}}\right) \mathrm{d}\left(\frac{1}{p^2}\right)$$

To include bremsstrahlung, Unsold (1955) extended the above range of integration, assuming that the 'binding' energy of free electrons is negative and has no bounds.

$$\sum_{p^*+1}^{\infty} \varepsilon_{B,p}^{\mathrm{ei}}(\nu, T_\mathrm{e})\, \mathrm{d}\nu\, \mathrm{d}\Omega = -\frac{1}{(4\pi\varepsilon_0)^2}\left(\frac{\mathrm{Ry}}{k_\mathrm{B} T_\mathrm{e}}\right)^{3/2} \frac{8e^4 h}{3m_\mathrm{e}^2 c^3 \sqrt{3\pi}} N_\mathrm{e} N_\mathrm{i} Z^4\, \bar{g}_\mathrm{ff} \exp\left(-\frac{h\nu}{k_\mathrm{B} T_\mathrm{e}}\right) \int_{-\infty}^{0} \exp\left(\frac{Z^2 Ry}{p^2 k_\mathrm{B} T_\mathrm{e}}\right) \mathrm{d}\left(\frac{1}{p^2}\right) \mathrm{d}\nu\, \mathrm{d}\Omega$$

thermally averaged free–free Gaunt factor

After integration

$$\varepsilon_B^{\mathrm{ei}}(\nu, T_\mathrm{e})\, \mathrm{d}\nu\, \mathrm{d}\Omega = \frac{16\pi e^6}{3c^3 (4\pi\varepsilon_0)^3 \sqrt{6\pi k_\mathrm{B} m_\mathrm{e}^3}} \frac{N_\mathrm{e}(x) N_\mathrm{i}(x, T_\mathrm{e})}{\sqrt{T_\mathrm{e}}} Z^2\, \bar{g}_\mathrm{ff}(\nu, T_\mathrm{e}) \exp\left(-\frac{h\nu}{k_\mathrm{B} T_\mathrm{e}}\right) \mathrm{d}\nu\, \mathrm{d}\Omega$$

The radiated power per unit volume (in W m^{-3})

$$P_B^{\mathrm{ei}}(T_\mathrm{e}) = \int_0^{4\pi} \int_0^{\infty} \varepsilon_\mathrm{B}^{\mathrm{ei}}(\nu, T_\mathrm{e})\, \mathrm{d}\nu\, \mathrm{d}\Omega$$

$$P_B^{\mathrm{ei}}(T_\mathrm{e}) = \frac{64 k_\mathrm{B} \pi^2 e^6}{3c^3 (4\pi\varepsilon_0)^3 h \sqrt{6\pi k_\mathrm{B} m_\mathrm{e}^3}} N_\mathrm{e}(x) N_\mathrm{i}(x, T_\mathrm{e}) Z^2 \bar{\bar{g}}_\mathrm{ff}(T_\mathrm{e}) \sqrt{T_\mathrm{e}}$$

total free–free Gaunt factor

Continua: comparison

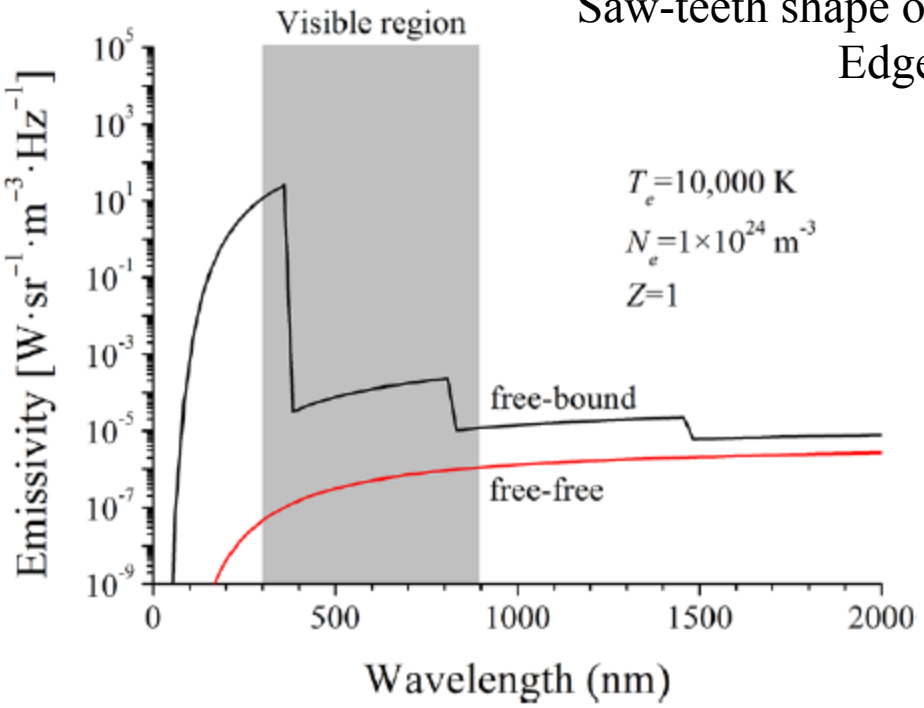

Saw-teeth shape of *f-b* emissivity Edges

$$P_R^{\mathrm{ei}}(T_\mathrm{e}) = \frac{256\pi^4 e^{10}}{3h^3c^3\sqrt{6m_\mathrm{e}\pi}}\frac{1}{(4\pi\varepsilon_0)^5}\frac{Z^4}{(k_\mathrm{B}T_\mathrm{e})^{1/2}}N_\mathrm{e}N_\mathrm{i}\sum_{\sqrt{\frac{Z^2\mathrm{Ry}}{h\nu}}}^{\infty}\frac{\bar{\bar{g}}_\mathrm{fb}}{p^3}\exp\left(\frac{Z^2Ry}{p^2k_\mathrm{B}T_\mathrm{e}}\right),$$

$$P_B^{\mathrm{ei}}(T_\mathrm{e}) = \frac{64k_\mathrm{B}\pi^2e^6}{3c^3(4\pi\varepsilon_0)^3h\sqrt{6\pi k_\mathrm{B}m_\mathrm{e}^3}}N_\mathrm{e}(x)N_\mathrm{i}(x,T_\mathrm{e})Z^2\bar{\bar{g}}_\mathrm{ff}(T_\mathrm{e})\sqrt{T_\mathrm{e}}$$

3. Observing and probing

Broadening and shift sources of emission lines

	Broadening	Potential	Line shape (Impact vs QS)		FWHM	Line shift
	Natural	NA	Gau.		$\Delta\nu_{\mathrm{L}} = \frac{1}{2\pi}[A_{u\rightarrow} + A_{l\rightarrow}]$	No
	Instrumental	NA	Lor.			No
	Doppler	NA	Gau.		$\Delta\nu_{\mathrm{D}} = \nu_0\sqrt{\frac{8\ln 2 \times RT}{Mc^2}}$	No
Pressure / Collisional	VdW	$V_6 = -C_6/r^6$	Lor.	Marg.	$\Delta\nu_{\mathrm{vdw}} = \left\|C_6'\right\|^{2/5}\bar{v}^{3/5}N$	Yes
Pressure / Collisional	L.J.	$V_{12} = C_{12}/r^{12} - C_6/r^6$				
Pressure / Collisional	Resonance	$V_3 = -C_3/r^3$	Lor. at low density		$\Delta\nu_{\mathrm{res}} = \pi k_{gl} C'_{3,gl}\sqrt{\frac{g_g}{g_l}}N_g$	
Pressure / Collisional	Stark lin.	$V_2 = -C_2/r^2$	Lor. e^- Holts. X^+		$\Delta\nu_s = 2\times10^{-22}\frac{\nu_0^2}{c}$ [$1 + 5.534\times10^{-6}N_e^{1/4}a(T_e)$ $(1 - 6.742\times10^{-3}\kappa N_e^{1/6}T_e^{-1/2})]N_e w_e(T_e)$	Yes
Pressure / Collisional	Stark quad.	$V_4 = -C_4/r^4$	Holts.			

High pressure

High Ne

4. Role of surfaces at HP

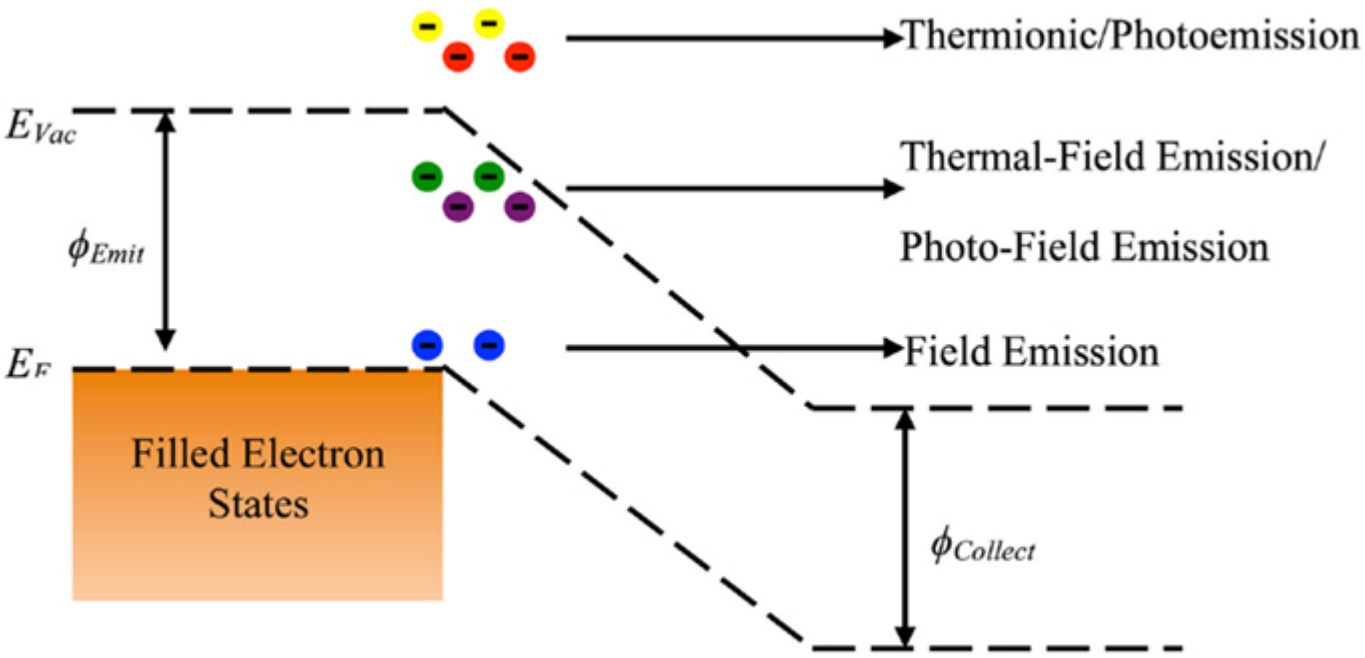

4. Role of surfaces at HP

Departure from Townsend's law at low gap

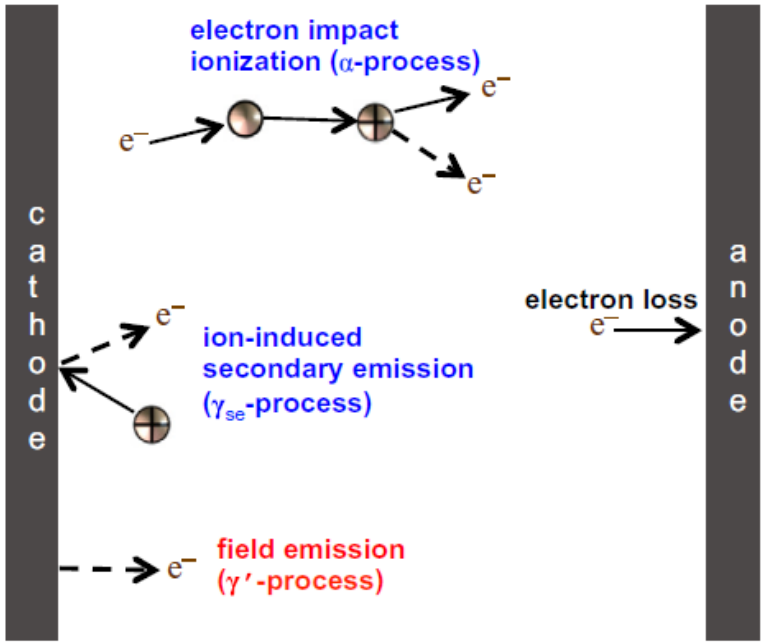

Schematic of charge generation processes in a standard DC discharge. Electron impact ionization (α-process) generates electrons in the volume while secondary emission (γ-process) generates electrons at the cathode. Field emission is the process of direct electron tunneling into the gas due to the high electric fields that are generated at the microscale.

Go and A Venkattraman, J. Phys. D: Appl. Phys. **47** (2014) 503001

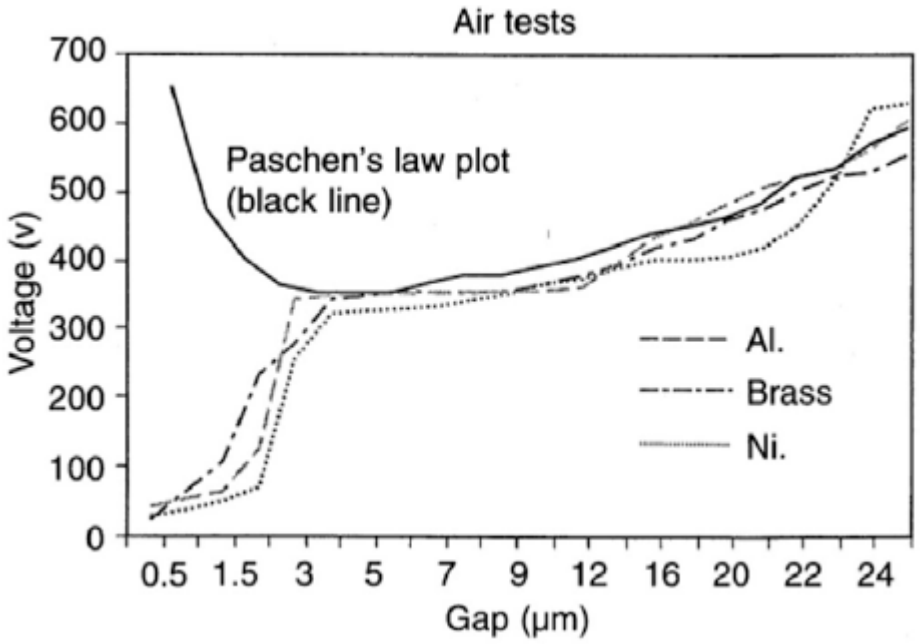

Plot of the breakdown voltage V_b as a function of the electrode gap spacing d for ambient air at atmospheric pressure using different cathode materials (aluminum-Al, brass and nickel-Ni)

Torres and Dhariwal, Microsys. Technol. **6** (1999) 6

4. Role of surfaces at HP

- For gaps ~ 1–10 μm near atmospheric pressure, field emission is a dominant process in the gas breakdown process : ~~Paschen's Law~~
- Field emission inherently couples to the discharge by responding to positive ions and positive space charge generated in the electrode gap, which increase the local electric field and lead to ion-enhanced field emission;
- Ion-enhanced field emission can be treated as an effective secondary emission coefficient γ' that has a functional dependance of $\gamma' = f(\exp(-1/E))$ and this over-exponential dependence on the electric field is the cause of deviations from Paschen's Law;
- Field emission's strong dependence on the electric field and thus the electrode gap causes standard pd scaling to fail, such that breakdown in microscale gaps is a function of p and d, separately.

4. Role of surfaces at HP

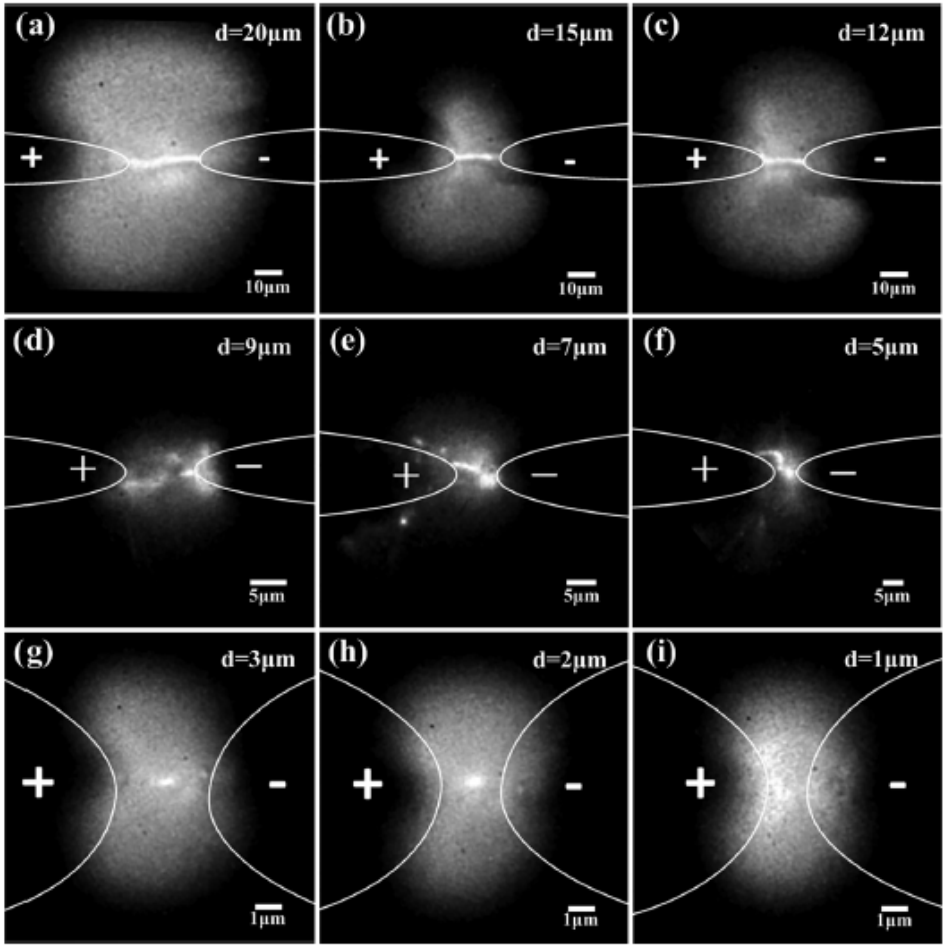

Meng and *al.*, PoP **25** (2018) 082116

Breakdown morphology at gap widths from 1 μm to 20 μm. (a)–(c) Show the breakdown propagating along the shortest path with luminescence filling the surrounding area, (d)–(f) show the roughly constant path lengths regardless of gap width which is consistent with the plateau of breakdown voltage in this region, and (g)–(i) indicate no obvious breakdown channel arising at these smallest gap distances.

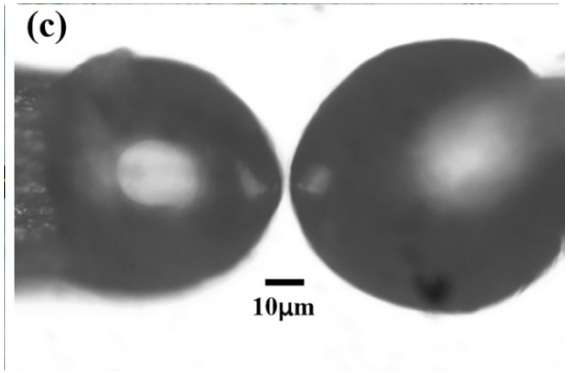

Picture of the inter-electrode gap

4. Role of surfaces at HP

For gap widths < 5-10 µm

1°) the initial electron avalanche is generated in the vicinity of the cathode tip

2°) The higher electric field reduces the potential barrier of the cathode enough for electrons to tunnel through and be released into the gap.

3°) The gap $d \sim \lambda_e$; therefore, the emitted electrons drift to the anode under the electric field and collide with the anode directly, heating the anode materials and the cathode due to the Nottingham effect* *(radiation heating might be non-negligible too)*

4°) Then, thermal electron emission would turn on and more electrons would be generated by the combination of field emission and thermal emission. The outgas and atoms would fill the gap, increasing the pressure. This causes a steep decline in breakdown voltage due to field emission.

Experimental data indicate the dominance of field emission as the breakdown mechanism for this range of gap widths.

* the cathode is cooled if the average energy of the emitted electrons is below the Fermi energy of the cathode material, otherwise electron emission contributes to the heating of the cathode.

4. Role of surfaces at HP

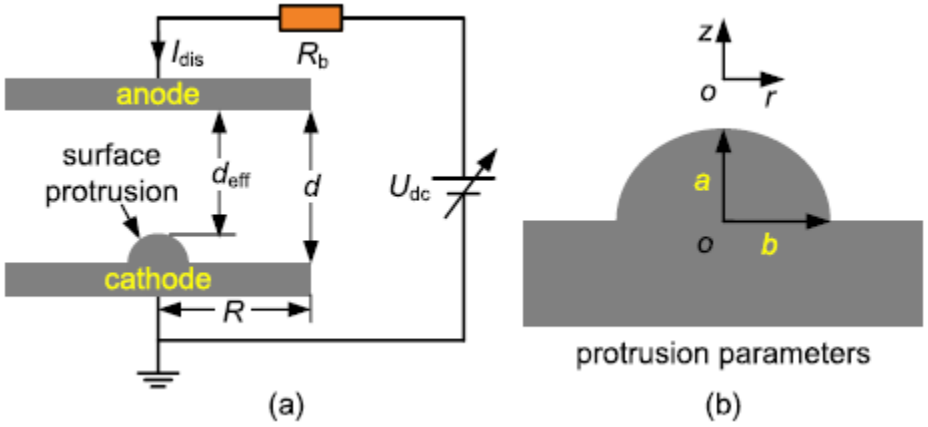

Schematic of the microdischarges. (a) The microgap with a DC voltage source Udc applied through a ballast resistor Rb while the cathode is grounded and (b) protrusion parameters: a is the axial dimension and b is the radial dimension.

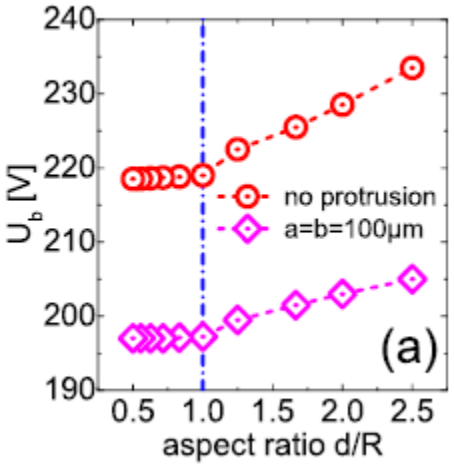

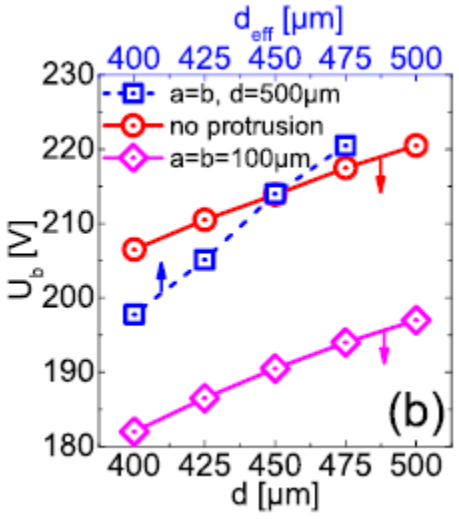

Geiger-Müller (G-M) regime

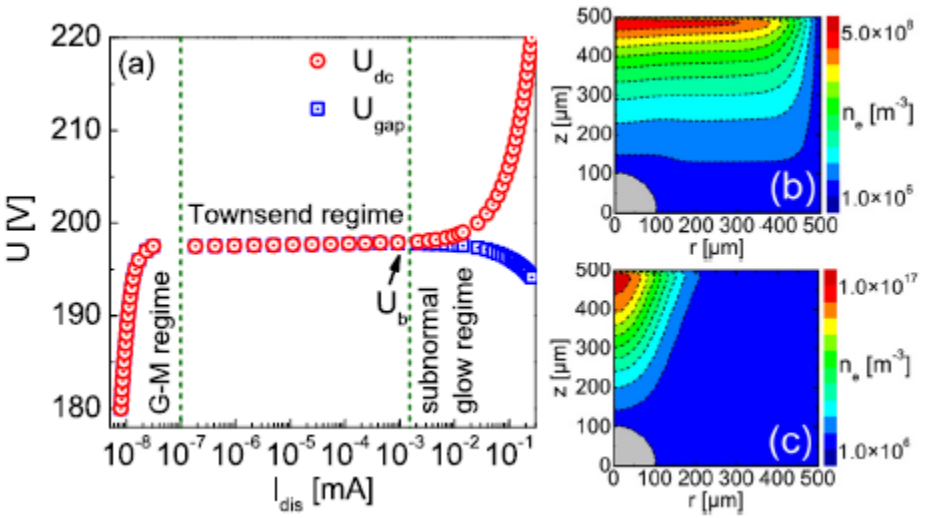

(a) The voltage-current characteristics for an atmospheric microgap with a cathode surface protrusion (a=b=100 μm) and the electron density distributions in (b) the G-M regime, and (c) the Townsend regime. In the simulation, we set R¼500 lm and d¼500 lm.

Fu, Zhang, and Verboncoeur, Appl. Phys. Lett. 112 (2018) 254102

(a) The effect of the microgap's aspect ratio d/R on the breakdown voltage in the microgap, with the gap distance d is fixed at 500 μm and the gap radius R increasing from 200 to 1000 μm, the aspect ratio ranging from 0.4 to 2.0 and (b) the breakdown voltage as a function of the effective distance d_{eff} and the gap distance d, for a fixed d/R = 1.0.

4. Role of surfaces at HP

Coupled electric, mechanical, thermal interactions

- Electric field deforms sample and causes emission currents
- Emission currents lead to current density distribution in the sample
- Material heating due to the electric currents
- Electric and thermal conductivity temperature and size dependent
- (Deformed) sample causes local field enhancement

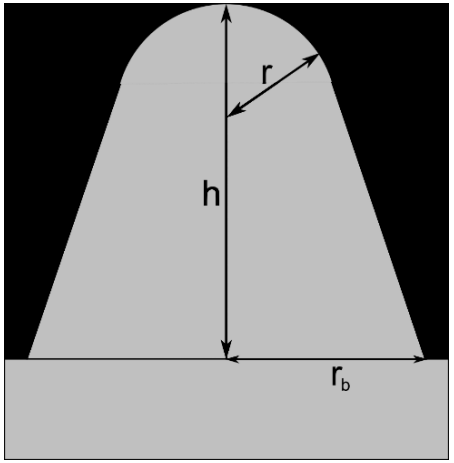

After V. Zadin
https://indico.cern.ch/

Institut Jean Lamour

CONCLUSION

1 – Les effets dus à l'élévation de la pression sont nombreux et nécessitent d'être pris en compte spécifiquement.

2 – La densification des plasmas à haute pression peut être contournée en diminuant les distances (cas des APGD par exemple) mais cela conduit à des contraintes… dimensionnelles.

3 – La physique et la chimie des milieux ionisés sous haute pression a beaucoup progressé, mais de nombreux aspects, notamment en relation avec les surfaces, nécessiteraient d'être approfondis (ectons, électron runaway dans des aspérités, processus de relaxations vibrationnels, etc.)

4 – Les diagnostics ont fortement progressé également, mais certains restent encore difficiles à implémenter ou à maîtriser pour disposer à la fois des résolutions spatiales, temporelles et spectrales.

5 – Au final, ne pas se contenter de changer la pression dans COMSOL pour simuler un plasma HP…

6. Conclusion

PLATHINIUM

PLASMA THIN FILM INTERNATIONAL UNION MEETING

23-27 September 2019

Antibes, French Riviera

SFV

Société Française du Vide

Thank you for your attention

Wei-wei's masterpiece